1969

The strength of welded flame-cut columns of astm A572 steel

Yoshio Kishima
Lehigh University

THE STRENGTH OF WELDED FLAME-CUT COLUMNS OF ASTM A572(50) STEEL

by

Yoshio Kishima

A Thesis
Presented to the Graduate Faculty
of Lehigh University
in Partial Fulfillment of the Requirements
for the Degree of
Master of Science in Civil Engineering

September 1969

This thesis is accepted and approved in partial fulfillment of the requirements for the degree of Master of Science.

12 September 1969
Date

Lambert Tall
Dr. Lambert Tall
Professor in Charge

David A. VanHorn
Dr. David A. VanHorn
Chairman
Department of Civil Engineering

THE STRENGTH OF WELDED FLAME-CUT COLUMNS OF ASTM A572 (50) STEEL

by Yoshio Kishima

ABSTRACT

This thesis describes the results of an extensive investigation into the strength and behavior of steel wide-flange columns welded from flame-cut plates. The material chosen for the study is ASTM A572 (Grade 50) steel.

Both experimental and theoretical studies are presented in this thesis. The column sections selected for the investigation are two welded wide-flange shapes manufactured from flame-cut plates, that is, 12H79 and 14H202 shapes. The experimental research includes tension specimen tests, residual stress measurements, stub column tests, and pinned-end column tests. Residual stress measurements were made on these welded shapes as well as on their component loose plates to determine the magnitude and distribution of actual residual stresses existing in the cross sections. Pinned-end columns were tested with end rotations limited about the weak axis, and for slenderness ratios of 30, 60, and 90.

The theoretical prediction of the column strength is in two parts. The first part is based on the tangent modulus load concept. Tangent modulus loads are computed for both weak axis and strong axis bendings. This computation utilizes the patterns of actually measured residual stresses in the cross sections. The second part of the column strength prediction is an ultimate strength analysis of a pinned-end column with respect to the weak axis. This analysis takes into account the actually measured residual stress pattern together with the initial out-of-straightness of the column.

The results obtained from the residual stress measurements show that very high tensile residual stresses exist in the region near the flange tips and at the web-to-flange juncture. This distribution gives a favorable effect on column strength. That is, both the pinned-end column tests and the tangent modulus load predictions show that welded flame-cut columns have high weak-axis column strength, especially in the lower slenderness ratios which are more important for practical columns. The tangent modulus load analysis shows that

the column strength is nearly identical about the strong and weak axes of the cross section for these wide-flnage columns welded from flame-cut plates. In other words, the effect of high tensile residual stress at flange tips on column strength is greater for "weak" axis bending than for "strong" axis bending.

The comparison of the test results with the analysis shows that the tangent modulus load gives a good estimate of the ultimate strength of these welded flame-cut columns.

The study indicates that the behavior of welded flame-cut columns of the newly-designated high-strength steel ASTM A572 (Grade 50) is very similar to that of similar columns of structural carbon steel, A36.

TABLE OF CONTENTS

1. INTRODUCTION

1.1 Previous Studies

After the significance of the effect of residual stress on the column strength had become known, the earlier work in the study of column strength was concerned with rolled shapes, and with residual stresses due to cooling after rolling. A summary report of such an investigation is Ref. 1.

(2-6)

Studies were commenced then on welded shapes built-up from universal-mill (UM) plates; these were of relatively small cross section. Welded H-shapes manufactured from UM plates have relatively high compressive residual stresses at the flange tips, which contributes to lower strength of such columns, when compared to that of similar rolled H columns.(1,7)

(7)

A pilot study on the strength of two steel columns welded from flame-cut plates; 6H27 and 10H61 shapes*, showed that these shapes had more

*"H" designates a welded H-shape, while "WF" is for a rolled wide-flange shape.

"favorable" residual stress distributions which would result in higher column strengths. Also, a column strength study for two welded flame-cut shapes; that is, 12H79 and 14H202 shapes, of ASTM A36 steel was conducted.[8] This is the study preceding the one presented in this thesis. It is noted from the study that welded flame-cut columns have relatively high weak-axis column strengths in the lower slenderness ratios. This is caused by the tensile residual stresses existing at the flange tips.

1.2 Purpose and Scope

The purpose of the study described in this thesis is to investigate the strength and behavior of medium size steel columns welded from flame-cut plates. Both the experimental study and the theoretical predictions were carried out for this purpose on two different shapes of ASTM A572 (Grade 50) steel.[9] The phases of the research are as follows:

1. Residual stress measurements in wide-flange shapes welded from flame-cut plates (Sects. 2.3, 3.3).

2. Residual stress measurements in component loose plates prior to welding.(Sects. 2.3, 3.2)

3. Experimental study of column strength including stub column tests (Sects. 2.4, 3.4) and pinned-end column tests with respect to the "weak axis".(Sects. 2.5, 3.5, and 5)

4. Theoretical prediction of column strength by means of tangent modulus concept (Sect. 4.2) as well as of ultimate load analysis.(Sect. 4.3)

Extensive studies into the strength of steel columns have been conducted in Fritz Engineering Laboratory, Lehigh University, Bethlehem, Pennsylvania. These studies have dealt with columns of various kinds of steels, yield point of steels ranging from 33 ksi. to 110 ksi., of various shapes and sizes of the cross sections, and of two different types of sections; rolled and welded shapes. For welded steel columns alone, there has been considerable research carried out on the

shapes built-up from both universal mill plates and flame-cut plates, see references, Chapter 10.

1.3 Manufacture and Fabrication

In the process of manufacturing the steel shapes welded from flame-cut plates, the material is subjected to various types of heat inputs which will produce different patterns of residual stresses in the cross section after the material has cooled. Generally, that material which cools last will contain tensile residual stresses.

The first heat input that affects the formation of residual stress is the rolling of plates. The temperature introduced in the plate during rolling is approximately 2,400°F. At the stage of cooling after rolling, compressive residual stresses are formed along the plate edges and tensile residual stresses in the center portion of the plate.

The second high heat input is introduced by flame-cutting of the plate, which is a local heat input to the plate. The flame-cutting creates tensile residual stress along the plate edges, being balanced by

compressive stresses present elsewhere in the plate. These stresses are superimposed on those due to rolling.

Finally, the welding of these flame-cut plates to form a shape causes additional residual stresses. Very high tensile stresses are formed in the vicinity of the weld, and compressive stresses elsewhere. The magnitude of residual stress due to welding reaches the yield stress of the weld material, as compared to rolled medium size wide-flange shapes in which the stresses are much smaller than the yield stress of the parent material.

2. DESCRIPTION OF TESTS

2.1 Test Material and Specimens

In the experimental phases of the study, four types of tests were carried out; tension specimen tests, stub column tests, residual stress measurements, and pinned-end column tests. The material is ASTM A572 (Grade 50) steel.[9] This has been newly designated by American Society for Testing and Materials, and is a high-strength low alloy columbium-vanadium steels of structural quality.

Two wide-flange shapes were chosen for the study; 12H79 and 14H202. Both are welded built-up shapes manufactured from flame-cut plates. The dimensions of these two sections are shown in Fig. 1. The dimensions of the shapes are determined so that they have counter-parts in the currently fabricated rolled wide-flange shapes. (In other words, 12WF79 and 14WF202 shapes exist.)

2.2 Tension Specimen Test

In order to determine the mechanical

properties of the material used, tension specimen tests were carried out. The number of tension specimens tested is shown in Table 1. Specimens were cut both from the H-section and the component loose plates for the 14H202 shape, and only from the shape itself for the 12H79 shape. The location of these specimens in the cross section is shown in Fig. 2 together with the dimensions of these tension test specimens. Figure 3 shows the layout of the specimens along the length of beams and plates. The testing machines used for the tension specimen tests are a mechanical testing machine of 120 kip capacity for the 12H79 specimens, and a hydraulic type machine of 300 kip capacity for the 14H202 specimens.

The results obtained include the complete stress-strain curves drawn by an automatic recorder. The data were evaluated for static yield stress (σ_{ys}),[10] strain at the onset of strain-hardening (ϵ_{st}), strain-hardening modulus (E_{st}), ultimate tensile stress (σ_u), percent elongation in 8 inch gage length, and percent reduction of area.

2.3 Residual Stress Measurement

For the determination of the magnitude and distribution of residual stress, the method of sectioning[11,12] was adopted using a Whittemore mechanical strain gage with a 10 inch gage length, which is shown in Fig. 4 together with a mild steel bar for the temperature compensation.

The method of sectioning requires at least two measurements of each gage length; once before sectioning, and then again after sectioning the specimen into strips. Furthermore, in this study, one additional step was included, which is called "partial sectioning". This is an intermediate step before "complete sectioning" as shown in Fig. 5. A smaller number of longitudinal cuttings are made for the partial sectioning (Fig. 5b) than for the complete sectioning (Fig. 5c). The purpose in doing this intermediate step is to have an approximate idea of the residual stress distribution and also to see if the number of sections can be reduced in future tests. Three repeated readings were taken at the time of all measurements.[13]

Thus, referring to Fig. 5, the steps of residual stress measurements are as follows:

1. Preparation of gage holes and layout of sectioning lines on the specimen.
2. Initial readings.
3. Transverse cutting. (Fig. 5a)
4. Partial sectioning. (Fig. 5b)
5. Readings after partial sectioning.
6. Complete sectioning. (Fig. 5c)
7. Final readings.

To evaluate residual stress from Whittemore gage readings, the following formula was used.

$$\sigma_{ri} = \frac{E}{L} [(\bar{B}_i - \overline{Ref.}\ \bar{B}_i) - (\bar{A}_i - \overline{Ref.}\ \bar{A}_i)]$$

where,

σ_{ri} = residual stress of the strip i (positive for tensile and negative for compressive residual stress),

E = modulus of elasticity,

L = gage length (equal to 10 inches for a Whittemore gage),

$\overline{B_i}$ = average of the initial readings on the strip i,

$\overline{Ref.B_i}$ = average of reference bar readings for the strip i before sectioning,

$\overline{A_i}$ = average reading on the strip i after sectioning,

$\overline{Ref.A_i}$ = average of reference bar readings for the strip i after sectioning.

The number of specimens used for residual stress measurements is given in Table 1. The location of the specimens in the fabricated column members and the component plates are shown in Fig. 3. The distances from the ends of the members to these sections were chosen to be at least one and a half times the largest linear dimension of the cross section. Thus, the stress existing in a long member was contained in the test specimen.[11]

The details of the sectioning are shown

in Figs. 6 and 7 for the 12H79 and 14H202 shapes, respectively. The location of the longitudinal cuts for the partial sectioning is also indicated in Fig. 7 for the shape 14H202. Figure 8 shows details of the partial and complete sectioning of the web (Fig. 8a) and the flange (Fig. 8b) loose plates.

2.4 Stub Column Test

In order to determine the average compressive stress-strain relationships of the complete cross section, stub column tests[14] were carried out for the two shapes, 12H79 and 14H202, of A572 (50) steel. The length of a stub column should be short enough to prevent column instability, yet long enough to have existing residual stress contained in the test specimen. The lengths of the stub columns tested were 3 ft. 6 in. for the 12H79 shape, and 5 ft. for the 14H202, their slenderness ratios being 13.8 and 14.8, respectively. Two identical stub columns were tested for both shapes, Table 1. The testing machine used for all four stub column tests was a hydraulic testing machine of 5,000 kip capacity, which has a set of beveled bearing plates built in it.

The test followed the procedure suggested by the CRC.[14]

Instrumentation

At the mid-height of the column on the centerline of the flanges, two dial gages with a sensitivity of 1/10,000 in. were mounted with a gage length of 10 in., one on each flange. They are for the determination of the average stress-strain curves. Four dial gages, with a sensitivity of 1/1,000 in., were fixed at each corner of the stub column, with a length the same as the complete length of the stub column specimen. These gages are utilized mainly for alignment of the stub column, as described below. In addition to these dial gages, there is set one more dial gage between the cross heads of the machine so that the test data can be recorded based upon the criterion of load stability after the load reaches the proportional limit. Furthermore, the specimen is whitewashed for easier judgement of the progress of yielding. The typical setup of the stub column in the testing machine is illustrated in Fig. 9, which is a 14H202 specimen.

Alignment

Prior to testing, the alignment was carried out for all stub columns, to make sure the load will be applied through the centroid of the cross section. The maximum alignment load was chosen to be approximately one half of the predicted yield load with the maximum compressive residual stress taken into consideration. The maximum alignment loads were 520 kips for the 12H79 specimens and 1,150 kips for the 14H202 specimens.

The alignment was achieved by observing the strain variation given by four corner dial gages. The criterion used for the alignment was such that the strain variation given by each one of the four corner gages should be less than 5% from their average value at the maximum alignment load. Six load increments were taken for all stub columns.

Testing

After the alignment condition was satisfied, testing was started with the load increments of 100 kips for the 12H79 specimens and 150 kips for

the 14H202 specimens, starting from zero load. By successively plotting the load-strain curve, and after the proportional limit (that is, the beginning of the derivation from the linear portion of the curve) was reached, the load increment was reduced so that the "knee" portion of the curve could be properly recorded.

When the load is bigger than the proportional limit, no readings were taken until the motion of the cross-head was stabilized. The criterion adopted for the stabilization was such that the movement of the cross-head, by checking the dial gage set in between the machine cross-heads, was less than 1/1,000 in. in a 2 minute interval.

Data Evaluation

The information evaluated from the stub column tests include modulus of elasticity (E), proportional limit (σ_p), yield strength (σ_{y1}), yield stress level (σ_{y2}), strain at the onset of strain-hardening (ϵ_{st}), and strain-hardening modulus (E_{st}). In evaluating the stub column test results, the method suggested by CRC was closely followed.[14]

2.5 Pinned-End Column Test

A total of five pinned-end columns were tested; three of the 12H79 shapes (L/r=30,60,and 90), and two of the 14H202 shapes (L/r=60 and 90). All tests were conducted as pinned-end about the weak axis and fixed-end about the strong axis. This was made possible by using the end fixtures with the cylindrical bearing surfaces developed in Fritz Engineering Laboratory.[15,16]

A hydraulic type universal testing machine with 5,000 kips capacity was used for all the pinned-end column tests.

Instrumentation

Prior to the testing, after all dimensions were measured, the following preparations and instrumentations were made on the column test pieces. (Fig. 10)

1. For the deflection measurements, strip scales were attached at several places along the column specimen. For relatively short columns, they were mounted at the quarter-points and at

both ends, and for longer columns, at the sixth-points and at both ends. Also, a theodolite was set on the testing floor some distance away from the column specimen to read these strip scales.

2. With the scales and theodolite, the initial out-of-straightness was measured for all the test columns.

3. In addition to the strip scales, one dial gage of 1/10,000 inch sensitivity was mounted at the mid-height of the column to measure the lateral deflection at that point, as the load increased.

4. SR-4 gages (electric resistance wire strain gages) were mounted at several positions; both ends and quarter-points or sixth-points depending on the column length. They were used to provide data for an indication of the strain distribution in these cross

sections at each load step for both alignment and testing. Four SR-4 gages were mounted at each level, except at the mid-height, where six gages were attached.

5. On one flange surface at the mid-height, three sets of gage holes were drilled for a Whittemore gage (Fig. 4) readings. This presents an additional indication of the mid-height strain.

6. In order to know the amount of pinned-end rotation, two level bars were mounted at both top and bottom end of the column. The level bar gives the measure of the angle changes by centering the level bubble with the micrometer screw at each loading step. The dial gage readings on the other end of the bar gives the end rotation of the bar over a 20 inch gage length.

7. One additional dial gage was set to

check the movement of the machine cross-heads. This was used to decide when to take all the readings once deflection commenced.

8. The column specimen was white-washed in order to have an indication of the yielding progress as the test proceeded.

Alignment

For all the columns tested, the alignment was made in the following manner. First of all, the column was geometrically centered in the testing machine. Then it was loaded to the maximum alignment load, which was smaller than the one for the stub column alignment, by taking reasonable load increments.

The alignment was based on the readings of the four corner gages at each cross section. Every effort was made, through many trial loadings, to achieve an alignment so that the deviation of any of these four corner gage readings was less than 5% from the average value of the four strains, at each of the three cross

sections; both ends and mid-height. When this was reached, the alignment of the column was considered to be satisfactory. Since the long column specimens tend to have some out-of-straightness, it was necessary to balance the eccentricity between the end sections and the mid-height section to achieve the alignment.(17)

Once alignment was attained, approximately 50 kips of load was left on the column specimen to protect it from any possible disturbances that might be caused in the fixtures or in the machine.

Testing

The column test was started from this initial load, and initial readings of all the gages and instruments were taken as zero readings.

The load increments were determined by simultaneously plotting a load-deflection curve as the test continued. This was especially helpful in the elastic-plastic region of the test.

In the elastic-plastic range and

thereafter, the cross head motion was carefully checked at each loading step in order to determine when to take readings. The criterion used for the stabilization was such that no reading was taken until there was no further perceptible movement of the machine cross heads over a three minutes interval.

3. TEST RESULTS

3.1 Mechanical Properties

The results obtained from tension specimen tests are summarized in Table 2, showing the values for static yield stress (σ_{ys}), ultimate tensile stress (σ_u), modulus of elasticity (E), strain-hardening modulus (E_{st}), strain at the onset of strain-hardening (ϵ_{st}), percent elongation in 8 inch gage length, and percent reduction of area. The material properties obtained from the tension specimen tests satisfied the ASTM requirements for A572 (Grade 50) steel.[9]

As can be seen from Table 2, for the values of percent elongation in an 8 inch gage length and of percent reduction of area, as well as from the specification, this low alloy high strength steel has a good ductility.

Average stress-strain curves using the average values of these data (E, σ_{ys}, ϵ_{st}, and E_{st})

are presented in Fig. 11 for both 12H79 and 14H202 shapes. The curve for the 14H202 shape shows a more gradual offset from the elastic range, a lower static yield stress, and an earlier onset of strain-hardening than the one for the 12H79 shape. This could be due to the effect of difference in size (see Fig. 2 for the dimensions of tension test specimens) and due to the small residual stresses left in the larger specimens cut from the 14H202 shape and from its component plates.

3.2 Residual Stresses in As-Manufactured Plates

Residual stress measurements were carried out on three loose plates taken from the same parent plate as the component plates of the 14H202 shape; one web plate (4D, 12 5/8" x 15/16") and two flange plates (4E and 4F, 15 3/4" x 1½").

The residual stress distributions measured for these plates are shown in Figs. 12, 13, and 14. Figure 12 shows the distribution of residual stress obtained for the web plate (4D) after partial sectioning (Fig. 12a) and after complete sectioning

(Fig. 12b). For the flange loose plate (4E and 4F), similar diagrams are given in Figs. 13 and 14.

Comparing the residual stress distributions corresponding to partial sectioning and complete sectioning on these three loose plates, it is noted that the partial sectioning procedure gives a good indication of the actual residual stress distribution, although only two cuts were made on each plate. Since the number of cuts and the number of measurements necessary for the partial sectioning is far less than what is required for the complete sectioning procedure, this suggests that accurate values at greater economy can be obtained by taking the step in between these two steps.

Relatively high tensile residual stresses exist at the flame-cut edges of the plates. These tensile stresses are balanced by an almost uniform compressive residual stress elsewhere in the plate. Some irregularity was observed in the distribution of residual stress at the edges of the flange plate 4E after complete sectioning as is seen in Fig. 13b. For

this plate, there appears to be a steep stress gradient across the plate thickness at the edges.

Summarizing the residual stress distribution in the component loose plates of the 14H202 shape of A572 (50) steel, Fig. 15, shows the average distribution in the web plate (4D, 12 5/8" x 15/16"). Average values were obtained from the stresses on both surfaces of the plate. The average tensile residual stress at the flame-cut edge is 43 ksi and the compressive residual stress in the mid-portion of the plate is approximately 4 ksi. These values correspond to 0.8 σ_{ys} and 0.07 σ_{ys}, respectively, where σ_{ys} is the static yield stress determined by tension specimen tests and is equal to 55.0 ksi for the web loose plate.

For the flange loose plates (4E and 4F, 15 3/4" x 1½") the similar distribution is shown in Fig. 16. The average tensile residual stress at the plate edge is 25 ksi and the compressive stress in mid-portion is approximately 3 ksi. They are 0.5 σ_{ys} and 0.06 σ_{ys}, respectively, where the static yield stress obtained from tension specimen tests is 53.0 ksi for the flange plates.

3.3 Residual Stresses in Welded H-Shapes

Residual stress measurements were also made on the two H-shapes welded from the flame-cut plates; 12H79 and 14H202.

Residual stress distributions obtained from three identical sections of the 12H79 shape of A572 (50) steel are shown in Figs. 17a, b, and c. As is seen in these diagrams, a very high tensile residual stress exists in the weld portion, and also at the flange tips due to the flame-cutting of plates. Compressive residual stresses are rather uniformly distributed elsewhere in the cross section to give equilibrium of the whole section. Although there is some irregularity in the upper right flange in Fig. 17b, the pattern of residual stress distribution is basically the same in all three sections. Since these three sections were cut originally from one long member, it may be noted that residual stress distribution is constant along the length of a member.

Figure 18 shows the average distribution of residual stress in the 12H79 shape of A572 (50) steel

together with the corresponding one in A36 steel.[8] Average stresses are calculated by taking one half of a flange and one half of a web as units. That is, each point in the flange represents the average of 24 stresses, and the one in the web represents 12 stresses measured, and the diagram shown is symmetrical about two axes. The average tensile residual stress for the A572 (50) steel shape is 15 ksi at the flange tip and 43 ksi at the weld, which corresponds to 0.3 σ_{ys} and 0.8 σ_{ys}, respectively, the average static yield stress (σ_{ys}) being 55.8 ksi for the shape, as shown in Table 2. The residual stress in mid-portion of the flange is approximately 15 ksi in compression, and the one in mid-portion of the web is about 4 ksi in tension, that is, 0.3 σ_{ys} and 0.06 σ_{ys}, respectively.

From Fig. 18, the residual stress distribution is very similar in both types of steel and so is the magnitude of residual stresses. This confirms[18] that the type of steel, or the yield point of steel, does not greatly affect the magnitude and the distribution of residual stress.

For the shape 14H202 of A572 (50) steel, the residual stress distributions measured are shown in Fig. 19a and b. These two sections were cut originally from one member. The tendency of the distribution is more or less similar to the one in a 12H79 shape. The main difference in the residual stress distribution in these two shapes is that the highest compressive residual stress exists on the outside surface of the flange at the web-to-flange juncture in the 14H202 shape, while in the 12H79 shape the corresponding point is in tension.

The average residual stress distributions in the 14H202 shape of both A572 (50) and A36 steels are illustrated in Fig. 20. Again the average stresses are computed on the basis of one half flange and one half web. That is, one point in the flange is the average of 16 stresses, and the one in the web represents 8 stresses measured for each steel.

The residual stress distribution is very similar to the one in 12H79 shape, and the pattern is similar for both A572 (50) and A36 steels. For the shape

of A572 (50) steel, the average tensile residual stresses are 20 ksi at the flange tip, and 27 ksi at the web-to-flange juncture. Since the average static yield stress determined from tension specimen tests is 54.0 ksi, they are 0.4 σ_{ys} and 0.5 σ_{ys}, respectively. The compressive residual stress is approximately 13 ksi in the mid-portion of the flange and 4 ksi in the mid-portion of the web, which correspond to 0.2 σ_{ys} and 0.08 σ_{ys}, respectively.

3.4 Stub Column Test Results

A total of four stub columns, two identical specimens for both shapes, 12H79 and 14H202, were tested in a hydraulic type universal testing machine with the capacity of 5,000 kips.

The load-strain curve obtained from one of the 12H79 stub columns is shown in Fig. 21, where the abscissa ϵ is the strain over the 10 inch gage length measured at the mid-height. The similar curve for one of the 14H202 stub columns is shown in Fig. 22. From these two curves, as is usually the case for a welded wide-flange stub column, there is no

obvious yield plateau in the curves. For two stub columns of the 14H202 shape, the machine capacity was not large enough to get the maximum load. Therefore, the testing was stopped at a load of 5,000 kips.

Both the 12H79 and 14H202 stub columns showed flange local buckling first, and then web local buckling. The final configuration of one of the 12H79 stub column is shown in Fig. 23, and one of the 14H202 shape in Fig. 24.

From the four stub column tests, the data were evaluated for modulus of elasticity (E), proportional limit (σ_p), yield strength (σ_{y1}), yield stress level (σ_{y2}), strain at the onset of strain-hardening (ϵ_{st}), and strain-hardening modulus (E_{st}). They are tabulated in Table 3, where, proportional limit (σ_p) is determined as the stress at an offset of 10 micro in./in. strain, yield strength (σ_{y1}) is the stress at 0.2% strain offset, and yield stress level (σ_{y2}) is the stress at 0.5% strain. The strain at the onset of strain-hardening is defined as the intersection of the yield stress level with the tangent of the curve

in the strain-hardening range. The terms of stub column properties are defined in Refs. (14) and (19), and the method of the data evaluation suggested by CRC[14] is adopted in this study.

3.5 Pinned-End Column Strength

A total of five column tests were conducted; three columns of the 12H79 shape and two of the 14H202 shape. All the columns were tested with end rotation limited about weak axis.

The initial out-of-straightness of these columns, measured by means of the strip scales and a theodolite, is illustrated in Fig. 25. The load-deflection curves obtained from the test of the 12H79 columns are shown in Fig. 26, and those of the 14H202 columns, in Fig. 27. All the curves in Figs. 26 and 27 indicate a relatively large deflection at loads near the maximum load.

The column test results are summarized also in Table 4, giving identification, length, L/r ratio, initial out-of-straightness, and the maximum

load for each of the five columns, with the predicted tangent modulus load. (See Sects. 4.2 and 5 for the tangent modulus load prediction.)

The final configurations of the five columns after the tests are shown in Figs. 28 through 32; Columns 3A, 3B and 3C of the 12H79 shapes are shown in Figs. 28, 29 and 30, respectively, and Columns 4B and 4A of the 14H202 shape, in Figs. 31 and 32, respectively.

4. THEORETICAL COLUMN STRENGTH STUDY

4.1 Brief Review

The buckling load prediction studied in this thesis was based on the tangent modulus load concept, taking into account the actually measured distribution of longitudinal residual stresses.

The tangent modulus concept was first proposed by Engesser in 1889, substituting the slope of the stress-strain curve by the tangent modulus at a point. In 1895, he modified the theory, and introduced the concept of "reduced modulus" which takes into account two moduli depending upon whether a fiber in the cross section is in the loading stage or in the unloading stage.

The reduced modulus theory had been regarded as the exact buckling theory for the centrally loaded columns until Shanley's paper[20] which gave the buckling load of a centrally loaded column based on the tangent modulus concept. He stated that the tangent modulus load was the lowest load at which bifurcation

could occur without strain reversal in the column cross section.

Since test results usually fall closer to the tangent modulus load than to the reduced modulus load, and since it is more convenient for design purpose, the modified tangent modulus load has been used to define column strength.[21]

4.2 Tangent Modulus Load Prediction

The critical load predictions were made for both 12H79 and 14H202 columns of A572 (50) steel, based on the tangent modulus concept. Column curves were obtained for both cases of bending; weak axis and strong axis bending. The assumptions made for the computations are the following.

1. The idealized elastic-perfectly-plastic stress-strain relationship is assumed so that the critical stress is given by the following equation.

$$\sigma_{cr} = \frac{\pi^2 E \frac{I_e}{I}}{\left(\frac{L}{r}\right)^2}$$

where,

σ_{cr} = critical stress corresponding to the ~~tangent~~ modulus load,

E = modulus of elasticity,

I = moment of inertia of the entire cross section,

I_e = moment of inertia of the elastic portion of the cross section,

L = column length,

r = radius of gyration, r_y for the weak axis and r_x for the strong axis bending.

This equation is applicable to any cross section with a symmetrical pattern of residual stress distribution.(22)

2. A symmetrical pattern of residual stress is used by taking the average values of the actually measured residual stresses. (See Fig. 18 for the 12H79 shape, and Fig. 20 for the 14H202 shape.)

3. The variation of residual stress across the thickness of the component plates is regarded to be negligible and to have no effect on the column strength. The average value of both surface stresses are used.

4. The material is assumed to be homogeneous.

5. The yield stress of the weld metal is considered to be the same as that of the parent material of the section.

6. The column is assumed to be initially straight, and the load is applied through the centroid of the cross sections.

7. Plain sections before loading remain plain after loading up to the critical load.

8. Upon buckling of the column, no strain reversal occurs.

For the computation of the tangent modulus load curves, it is advisable to have as small a segment

as possible for the input data of the residual stress, in order to have a smooth curve. The systems of elements used in this study are the same as those used in the sectioning process, Figs. 6 and 7.

The computer program[23] was written in FORTRAN IV language and a CDC 6400 digital computer was used.

The results of this analysis are discussed in the following chapter, and the comparison is made with the results obtained from the previous study in A36, as well as with the test results.

4.3 Ultimate Strength Prediction

The ultimate strength is also predicted for one column of the 14H202 shape; column 4B (L/r = 60), and only for the case of weak axis bending.

A computer program was developed to calculate the load-deflection curve for any H-shape column. This computation is based on the tangent modulus concept assuming an idealized elastic-perfectly-plastic stress-strain relationship for all the fibers

in the cross section. The symmetrical pattern of residual stress distribution was used taking one half of a flange and one half of a web as units. The variation of residual stress through the thickness of the plates was regarded to be negligible, and the average of the both surface residual stresses measured was used. The actually measured initial out-of-straightness was taken into consideration. That is, on a step-by-step process of computing a load-deflection curve, equilibrium of the cross section was checked at the one-eighth levels and at both ends, where the initial out-of-straightness was measured prior to the testing.

The theoretical result is presented in Chapter 5, and compared with the test result.

5. DISCUSSION OF COLUMN STRENGTH

The tangent modulus curves computed for the 12H79 shape columns are shown in Fig. 33 for weak axis bending, for the shape of A572 (50) steel and A36 steel.[8] Also shown in the figure are the test results of the three pinned-end columns of A572 (50) steel. (See Table 4) Comparison of these two curves shows that in the high slenderness ratio region, the A572 (50) steel column has a considerably larger strength than the A36 steel column; by as much as 20% at the maximum. This is due both to the difference in the yield stress of the two materials, and to the fact that the A36 shape has a compressive residual stress of about 10 ksi in the mid-web, while the A572 (50) shape has tensile residula stresses of approximately 4 ksi. (Fig. 18) Also, the A36 column curve has a higher strength level over a wide range of slenderness ratio, when compared to the A572 (50) curves. This is explained again by the difference in the residual stress distribution in both shapes; that of A36 steel has the larger area in the cross section with tensile residual stress; this helps the column sustain the higher load. Test points

indicate generally a good agreement with the predicted tangent modulus loads.

In Fig. 34, a similar diagram is shown for the larger 14H202 shape. The general shapes are similar to those of the 12H79 column curves. The difference in strength in the region of high slenderness ratio is smaller here than the previous case. This is due to the residual stress pattern. From Fig. 20, it is seen that, in the web, the residual stress pattern in the A36 steel shape has a steeper slope than the A572 (50) shape, towards the juncture of web-to-flange which slows the rate of yielding as the column is loaded. The computed tangent modulus load, again, gives a good prediction for the maximum strength of the welded flame-cut columns of A572 (50) steel.

All the four curves shown in Figs. 33 and 34 indicate a rather sudden rise approximately at L/r of 60 as the slenderness ratio decreases. This is typical for an H-shape column welded from flame-cut plates.[8]

As for the strong axis bending case, the

computed tangent modulus load curve for the 12H79 shape of A572 (50) steel is shown in Fig. 35 together with the one of A36 steel. Both curves show a more gradual increase in strength, with the decreasing slenderness ratio, than those of the weak axis bending. This is one phase of the strength of the welded flame-cut column which has high tensile residual stress at the flange tips. The difference in strength between the A572 (50) column and the A36 column is larger in high slenderness ratio range than in low slenderness ratio range, for the same reasons as described above.

Figure 36 shows the tangent modulus load curves for the 14H202 shape bent about strong axis. The shape of the curve is basically the same as the one for the 12H79 columns.

For both weak and strong axis bending cases, the difference in tangent modulus load in high slenderness ratio region is larger for the 12H79 shape than the 14H202 shape. In the range of low slenderness ratio, of L/r of less than about 20, the curve may not be precise, and may be conservative, since the strain-

hardening phenomenon takes place, and is not considered in this analysis.

Figure 37 shows the tangent modulus load curves for the 12H79 shape of A572 (50) computed for both cases of strong and weak axis bending. The similar one for the 14H202 shape is given in Fig. 38. From these two figures, it is noticed that the tangent modulus loads for both weak and strong axis bending are almost identical for the columns welded from flame-cut plates. In other words, the influence of tensile residual stress present near the flange tips upon the column strength is greater for the case of weak axis bending than for strong axis bending. For the 14H202 column of the mid-slenderness ratio (L/r of about 50), in particular, the "weak" axis strength is higher than the "strong" axis one. Therefore, for the welded flame-cut columns, the names of "strong" and "weak" axis column strength are merely conventional ones, and do not really imply strength.

As seen in Figs. 33 and 34, the tangent modulus load prediction gives a good estimate of the maximum strength of these H-columns built-up from flame-cut plates.

An ultimate strength prediction was prepared for column 4B, a 14H202 column of A572 (50) steel, with an L/r of 60. The predicted load-deflection curve for the column is shown in Fig. 39 together with the test results. The predicted maximum load was 2,370 kips, and from the test, the maximum load was 2,520 kips. A reason for this difference lies in the condition of load application. For the prediction, the load was assumed to be applied through the centroid of both end sections. However, the test column had an initial out-of-straightness (Fig. 25) and the alignment was made in such a way that three sections, mid-height and both ends, were loaded as uniformly as possible. Therefore, the point of load application was different in the test and the analysis, giving the lower load for the prediction by approximately 6% of the test result.

In Fig. 40, the progress of the lateral deflection of the same column is illustrated for both theoretical and experimental results. They are computed, and measured by strip scales and a theodolite, at one-eighth levels. The predicted deflection is in good agreement with the test result, although the loading stages are not the same for both.

6. SUMMARY AND CONCLUSIONS

This thesis presents the results obtained from a theoretical and an experimental study into the strength and behavior of the welded columns of A572 (Grade 50) steel, built-up from flame-cut plates. Tests were conducted on two sizes of the welded flame-cut columns; 12H79 and 14H202. The conclusions drawn from the study are as follows:

1. A very high tensile residual stress exists in the weld portion, and also at the flange tips of the welded flame-cut column section, showing the direct influence of welding and flame-cutting. Compressive residual stresses are rather uniformly distributed elsewhere in the cross section. (Section 3.3; Figs. 15, 16, 19, and 20).

2. The study confirmed that the residual stress distribution is constant along the length of a member. (Section 3.3; Figs. 3, 15, and 16).

3. Comparison of the residual stresses in A572 (50) steel shape and in A36 steel shape shows that the yield stress of the material has almost no effect on the magnitude and distribution of residual stress. (Section 3.3; Figs. 19 and 20).

4. For the columns of high slenderness ratios (approximately L/r of 60 or more), the A572 (50) steel column has a considerably larger strength than the A36 steel column. This is due both to the difference in the yield stress, and to the residual stress distribution. This is true for both weak axis and strong axis bending. (Chapter 5; Figs. 33-36).

5. This difference in the tangent modulus curves between the A572 (50) steel shape and the A36 steel shape is greater for the smaller shape (12H79) than for the larger shape (14H202). (Chapter 5; Figs. 33-36).

6. Tangent modulus load curves for the welded flame-cut columns bent about weak axis indicate a rather sudden rise, approximately at L/r of 60, as the slenderness ratio decreases. This rise is more gradual for the case of strong axis bending. (Chapter 5; Figs. 33-36).

7. Tangent modulus loads for both "weak" and "strong" axis bending are almost identical for the A572 (50) steel columns welded from flame-cut plates. (Chapter 5; Figs. 37 and 38).

8. The effect of tensile residual stress present near the flange tips upon the column strength is greater for "weak" axis bending than for "strong" axis bending. (Chapter 5; Figs. 37 and 38).

9. The tangent modulus load generally gives a good estimate of the maximum strength of welded flame-cut columns. (Chapter 5; Figs. 33 and 34).

10. The tensile residual stresses present at the flange tips are beneficial to column strength. This confirms earlier findings for lower strength steels. (Chapter 5; Figs. 33-38).

7. NOMENCLATURE AND DEFINITIONS

$\bar{A}_i$	Average readings of the gage length i after sectioning
b	Width of a flange
$\bar{B}_i$	Average readings of the gage length i before sectioning
E	Modulus of elasticity
E_{st}	Strain-hardening modulus
FC	Flame-cut
H	Welded wide-flange shape
I	Moment of inertia of the entire cross section
I_e	Moment of inertia of the elastic portion of the cross section
L	Gage length, Column length
P	Load

P_{max}	Maximum load obtained from column test
P_t	Predicted tangent modulus load
P_y	Yield load of the cross section
r	Radius of gyration
r_x	Radius of gyration with respect to strong axis
r_y	Radius of gyration with respect to weak axis
$\overline{\text{Ref. } A}_i$	Average of reference bar readings for the strip i after sectioning
$\overline{\text{Ref. } B}_i$	Average of reference bar readings for the strip i before sectioning
UM	Universal-mill
WF	Rolled wide-flange shape
δ	Column deflection, Initial out-of-straightness
ϵ	Strain
ϵ_{st}	Strain at the onset of strain-hardening.

σ_{cr}	Critical stress corresponding to the tangent modulus load
σ_p	Proportional limit
σ_{ri}	Residual stress of the strip i (positive for tensile and negative for compressive residual stress)
σ_u	Ultimate tensile stress
σ_{yl}	Yield strength
σ_{y2}	Yield stress level
σ_{ys}	Static yield stress
ASCE	American Society of Civil Engineers
ASTM	American Society for Testing and Materials
AWS	American Welding Society
CRC	Column Research Council, Engineering Foundation
ft.	Foot
in.	Inch

kips 1,000 lbs.

ksi kips per square inch

Onset of strain-hardening (ϵ_{st}) is the strain corresponding to the intersection of the yield stress level with the tangent of the stress-strain curve in the strain-hardening range.

Proportional limit (σ_p) is the stress at an offset of 10 micro in./in. strain.

Static yield stress (σ_{ys}) is the stress corresponding to the strain of 0.5% with zero strain rate.

Yield strength (σ_{y1}) is the stress at 0.2% strain offset.

Yield stress level (σ_{y2}) is the stress corresponding to the 0.5% strain.

8. ACKNOWLEDGEMENTS

This thesis presents the results of an investigation into the strength and behavior of steel wide-flange columns welded from flame-cut plates.

The research was conducted at Fritz Engineering Laboratory of Lehigh University, Bethlehem, Pennsylvania. Dr. Lynn S. Beedle is the Director of the Laboratory, and Dr. David A. VanHorn is the Chairman of the Civil Engineering Department.

The author owes his special thanks to Dr. Lambert Tall, director of the overall research program, who supervised the research and the preparation of this thesis. His thoughtful guidance and encouragement throughout the research program are sincerely appreciated. Appreciation is also due Dr. Göran A. Alpsten who was co-director of the study.

The research was sponsored by the American Iron and Steel Institute. The technical guidance provided by the members of Task Group 1 of the

the Column Research Council under the chairmanship of Mr. John A. Gilligan, is gratefully acknowledged.

The author also owes special thanks to his research colleagues, and in particular to Jacques Brozzetti, for their advice and assistance throughout the study.

The author is most grateful to Kenneth R. Harpel, Laboratory Superintendent, and his staff for their cooperation in conducting the various experiments.

The author also wishes to express his sincere appreciation to Richard N. Sopko for his fine work on the photographs, to John Gera and Mrs. Sharon Balogh for the preparation of all drawings, and to Miss Joanne Mies for her care in typing the entire manuscript.

9. TABLES AND FIGURES

Table 1 Number of Test Specimens

Types of Tests \ Shape		12H79 (FC)	14H202 (FC)
Tension Specimen	Flange	12	9*
	Web	3	3**
Residual Stress Measurement	Shape	3	2
	Plate	0	3
Stub Column		2	2
Pinned-End Column (Weak Axis)	L/r=30	1	0
	L/r=60	1	1
	L/r=90	1	1

* 3 specimens are cut from the shape, 6 from the flange loose plates.

** 1 specimen is cut from the shape, 2 from the web loose plate.

Table 2 Tension Sepcimen Test Results

Shape or Plate	Specimen No.	Static Yield Stress (ksi)	Modulus of Elasticity (10^3 ksi)	Ultimate Stress (ksi)	Strain* at Strain-Hardening (%)	Strain-Hardening* Modulus (ksi)	Elongation in 8 in. Gage Length (%)	Reduction of Area (%)
Shape 12H79 (Flange)	3A1	55.3	29.9	85.6	—	—	24.8	45.0
	3A2	57.2	29.7	85.8	1.10	748	25.6	48.9
	3A4	54.0	31.2	82.8	1.05	698	26.5	50.3
	3A5	54.8	28.6	82.6	1.14	710	25.8	52.4
	3B1	55.5	28.7	84.9	1.07	691	26.0	47.9
	3B2	56.7	20.4	85.0	1.58	411**	25.3	47.9
	3B4	54.2	29.8	84.4	1.00	676	25.3	47.7
	3B5	54.9	29.5	82.6	1.12	685	26.4	51.3
	3C1	56.7	30.2	86.1	0.80	712	23.9	46.6
	3C2	56.7	28.6	85.6	1.01	728	24.5	46.8
	3C4	57.1	28.8	86.9	0.86	777	22.3	44.9
	3C5	57.3	28.4	87.2	0.90	758	20.5	44.8
Flange Average		55.9	—	85.0	1.06	719	24.7	47.9
Shape 12H79 (Web)	3A3	56.5	30.8	74.6	1.83	436	22.8	46.1
	3B3	54.6	18.2	78.2	—	—	27.1	48.1
	3C3	55.6	28.0	73.2	1.97	506	25.8	48.8
Web Average		55.6	—	75.4	1.90	471	25.2	47.7
Average ‡		55.8	—	82.7	1.25	662	24.8	47.9
Shape 14H202 (Web)	4B1	55.3	22.3	86.5	—	823	26.5	56.5
	4B2	55.1	28.5	86.6	0.86	859	27.0	56.8
	4B3	55.0	27.0	86.0	—	840	23.8	40.7
Flange Loose Plate	4E1	51.4	29.3	83.6	0.63	771	27.2	58.8
	4E2	52.4	29.3	83.7	0.67	836	26.7	58.7
	4E3	52.6	28.2	84.7	0.63	839	26.6	56.8
	4F1	53.9	29.7	84.4	0.50	836	27.8	58.1
	4F2	—	26.4	85.0	0.53	808	26.9	57.0
	4F3	54.5	30.2	85.1	0.44	849	26.5	56.6
Flange Average		53.8	—	85.1	0.61	829	26.6	55.6
14H202 (Web)	4B4	54.0	—	80.8	1.04	723	26.9	56.6
Web Loose Plate	4D1	54.7	28.8	84.5	0.76	796	22.6	49.3
	4D2	55.3	29.5	84.2	0.72	714	23.6	50.1
Web Average		54.7	—	83.2	0.84	744	24.4	52.0
Average ‡		54.0	—	84.7	0.65	811	26.1	54.8

* Estimated from load-elongation diagrams drawn by an automatic recorder.

** Omitted when averaging

‡ Weighted average

Table 3 Stub Column Test Results -- A572 (50) Steel

	12H79(FC)			14H202(FC)		
	ST-3B	ST-3C	Average	ST-4B	ST-4C	Average
Modulus of Elasticity x10^3, ksi *	28.8	31.1	29.9	33.5	30.5	32.0
Proportional Limit,ksi	38.3	46.8	42.6	37.2	39.0	38.1
Yield Strength,ksi	53.2	53.2	53.2	55.7	58.2	57.0
Yield Stress Level,ksi	53.8	54.4	54.1	58.7	59.3	59.0
Strain at the onset of Strain-Hardening,%	0.45	0.80	0.63	0.32	0.42	0.37
Strain-Hardening Modulus, ksi *	538	632	585	985	912	949

*Estimated from the load-strain curve.

Table 4 Pinned-End Column Test Results -- A572(50) Steel

Shape	Identification Number	L (ft-in)	L/r_y	Initial Out-of-Straightness					Column Strength		
				At Mid-Height		Max δ			P_{max} (kips)	P_{max}/P_y	P_t/P_y
				δ (in)	δ/b	δmax(in)	Location	δmax/b			
12H79 (FC)	3A	7'-8"	30	0.02	0.0016	0.03	1/4	0.0025	1,184	0.90	0.92
	3B	15'-3"	60	0.16	0.013	0.20	1/3	0.016	995	0.76	0.76
	3C	22'-10"	90	0.02	0.0016	0.06	1/6	0.005	780	0.60	0.66
14H202 (FC)	4B	20'-4"	60	0.11	0.007	0.14	1/4	0.009	2,520	0.80	0.79
	4A	30'-6"	90	0.27	0.017	0.31	1/3	0.020	1,912	0.61	0.68

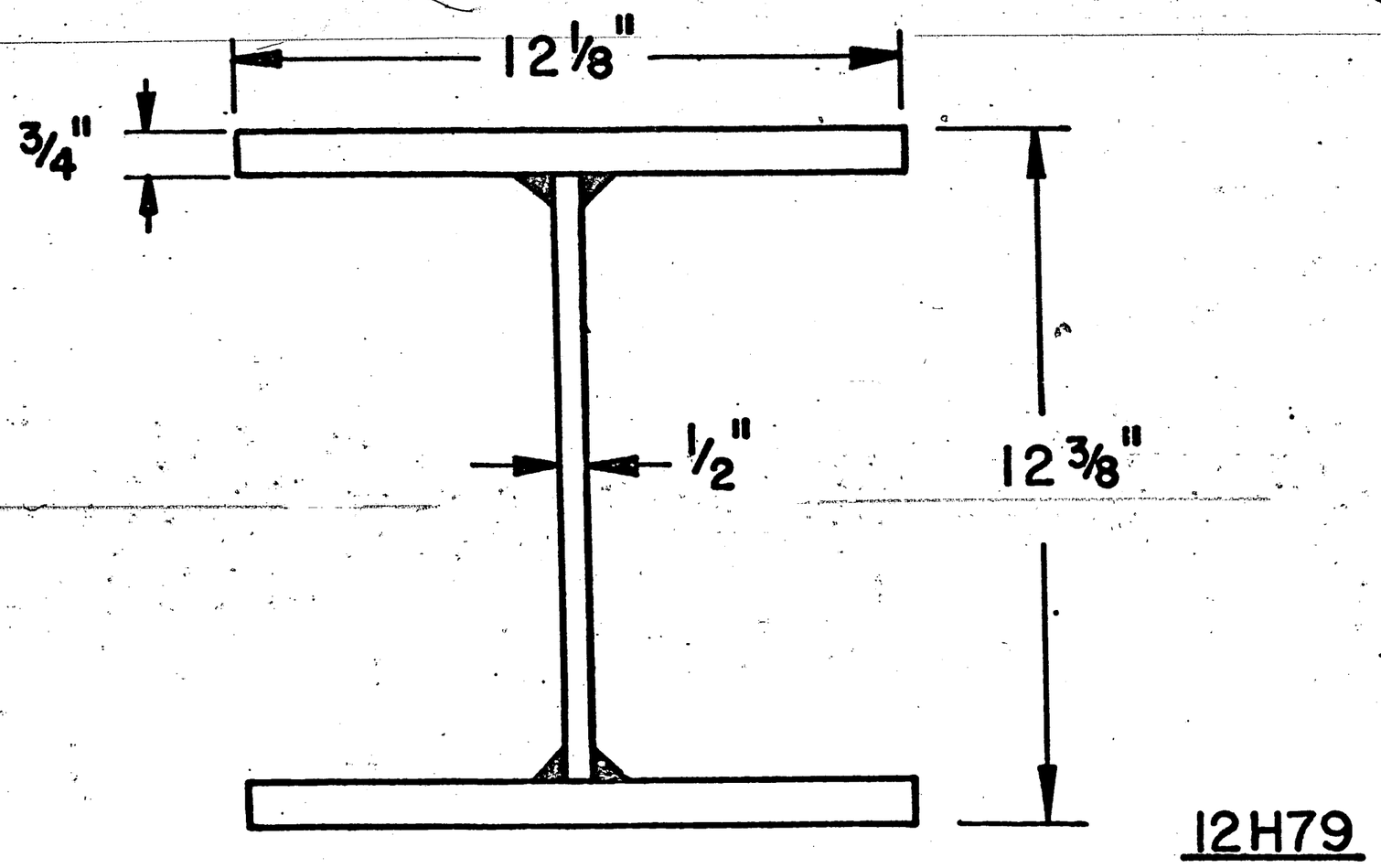

Fig. 1 Dimensions of the Shapes Studied

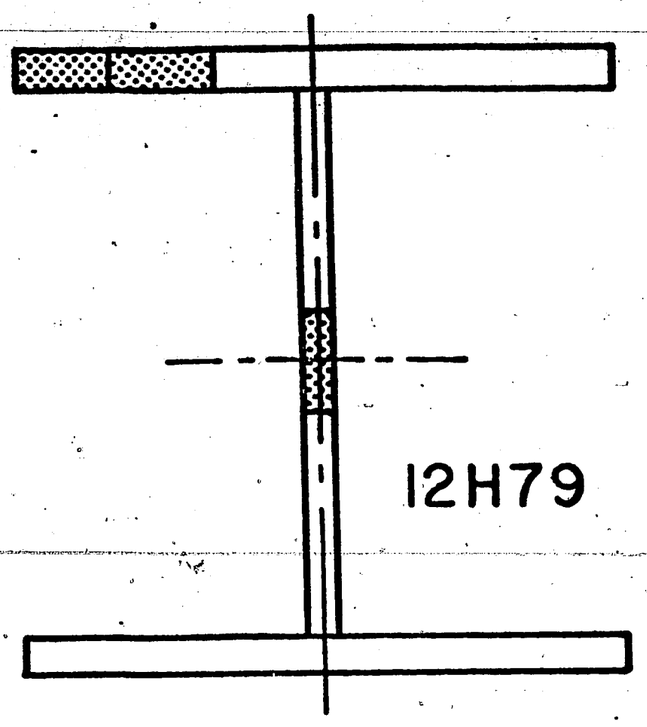

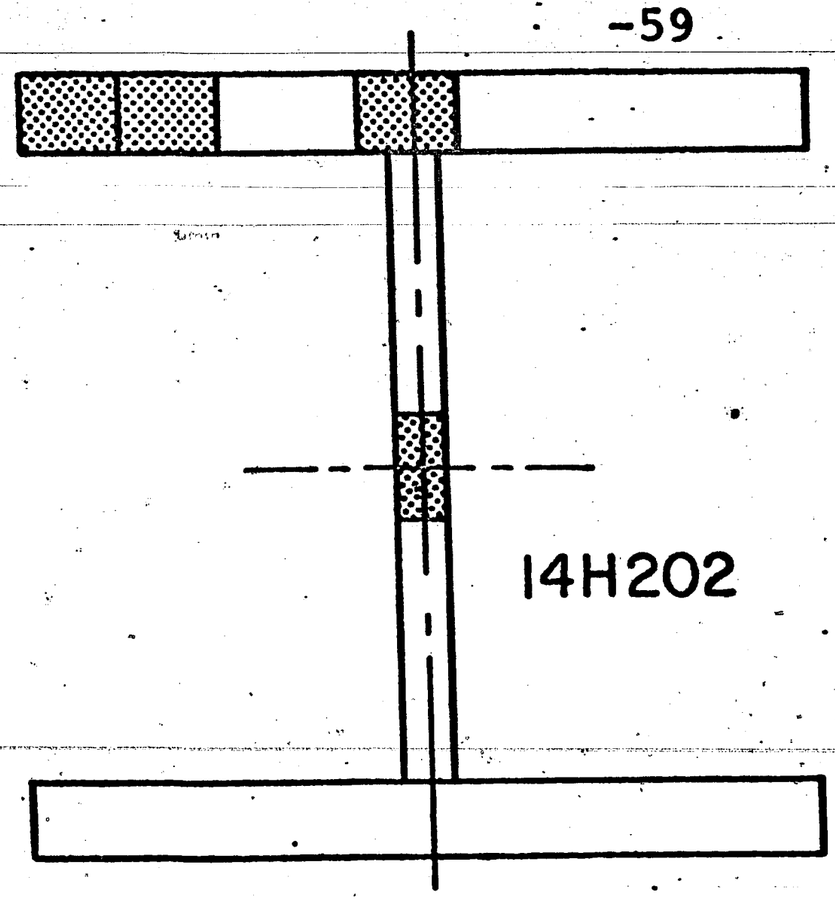

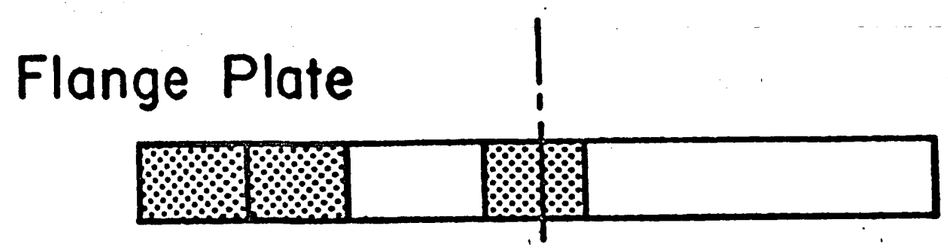

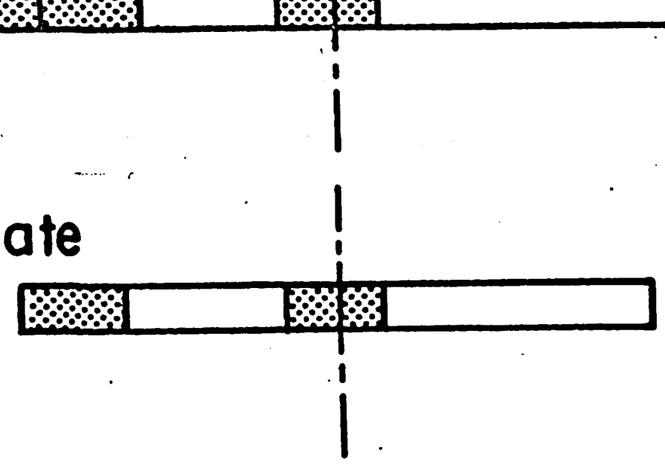

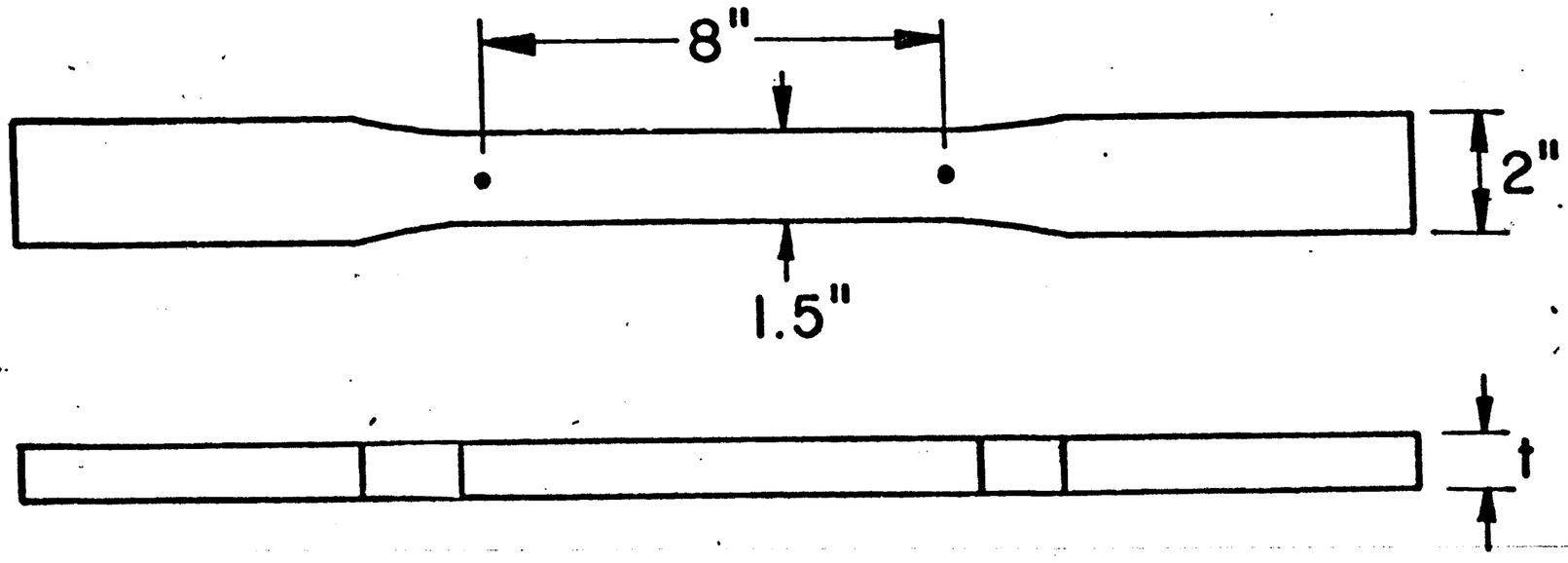

	12H79		14H202	
	Flange	Web	Flange	Web
t	3/4"	1/2"	1 1/2"	15/16"

Fig. 2 Location of Tension Test Specimens in Cross Sections

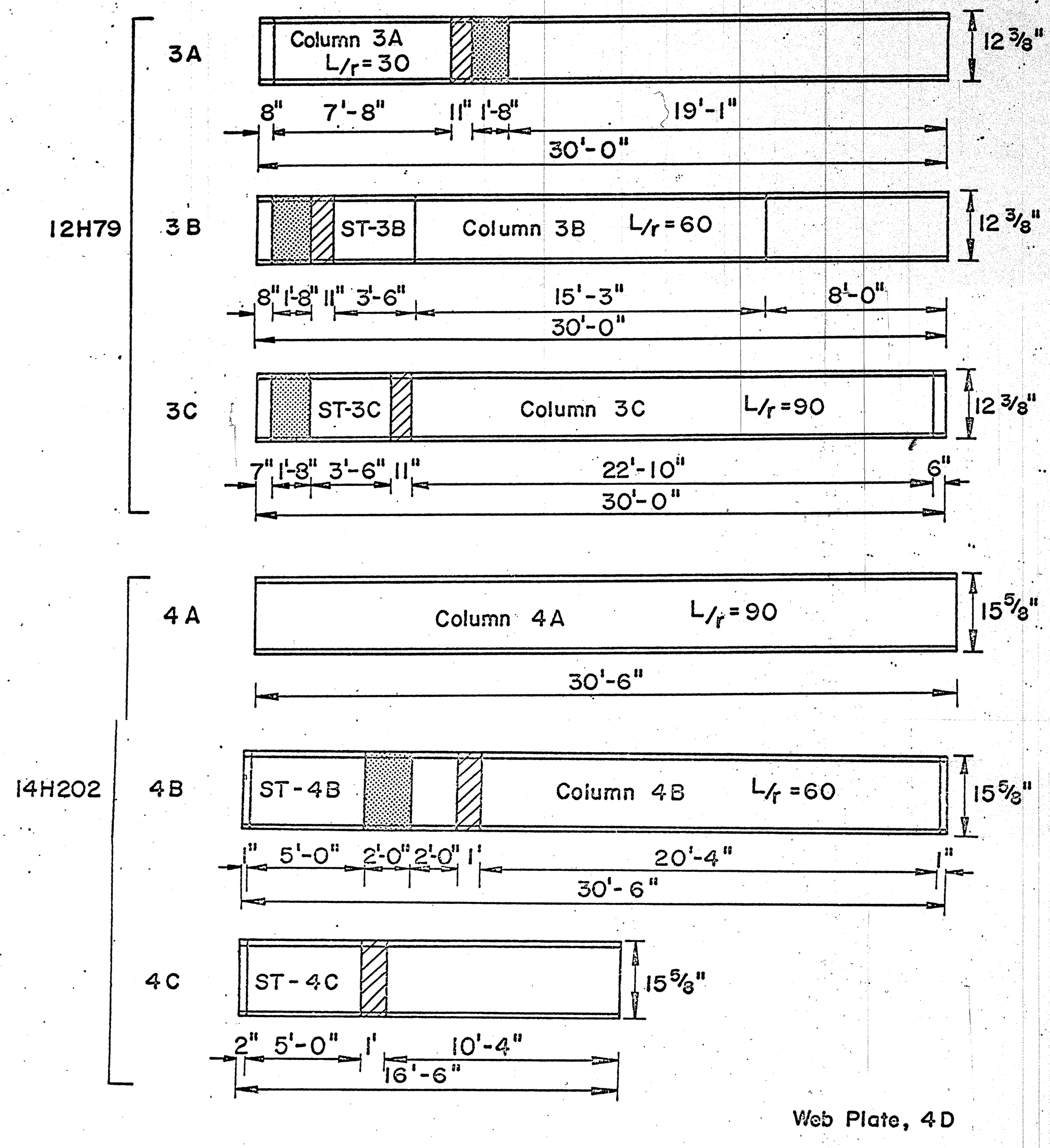

▨ Specimens for Residual Stress Measurements

▩ Tension Test Specimens

Fig. 3 Layout of Test Specimens

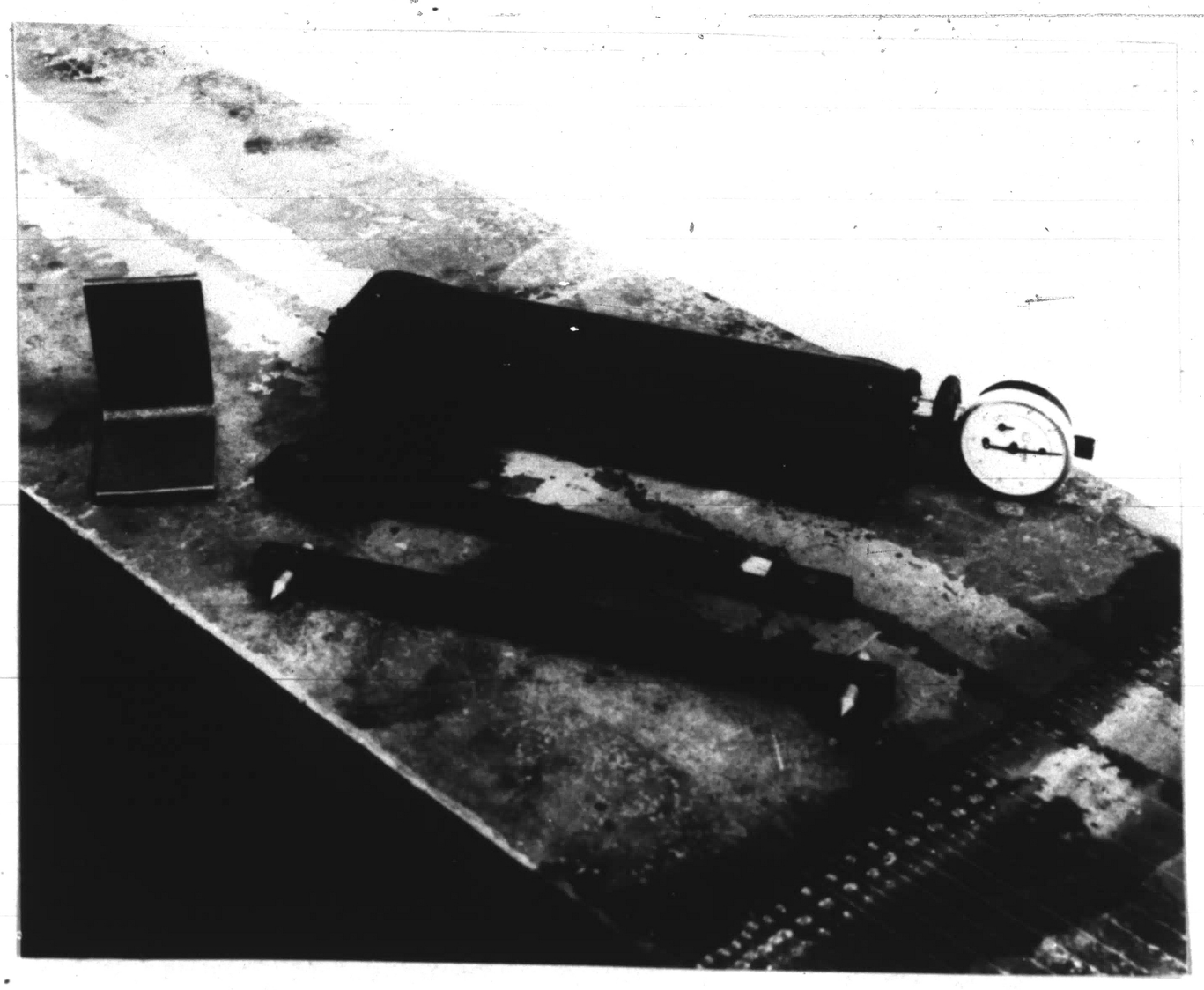

Fig. 4 Whittemore Strain Gage

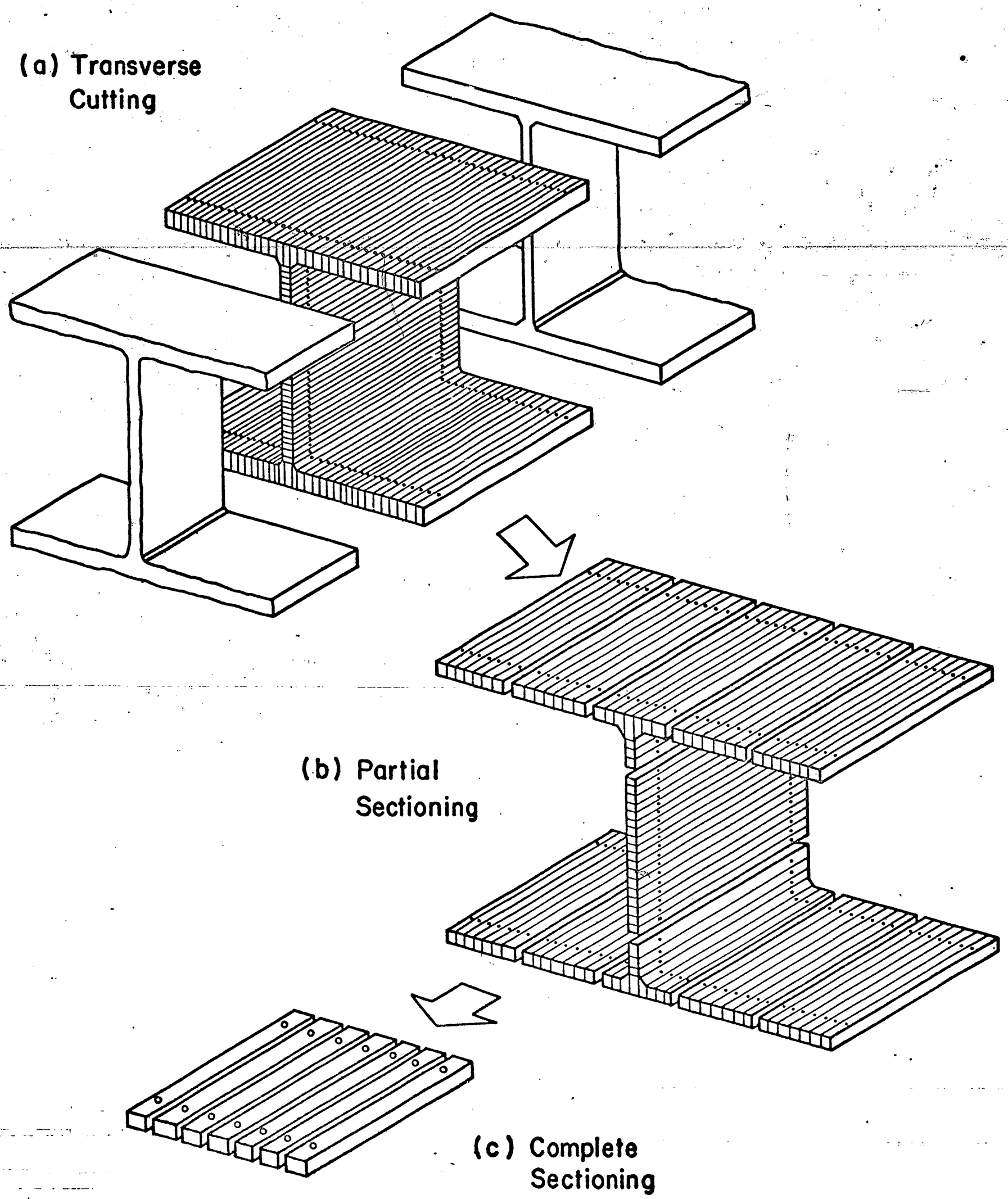

Fig. 5 Sectioning Steps

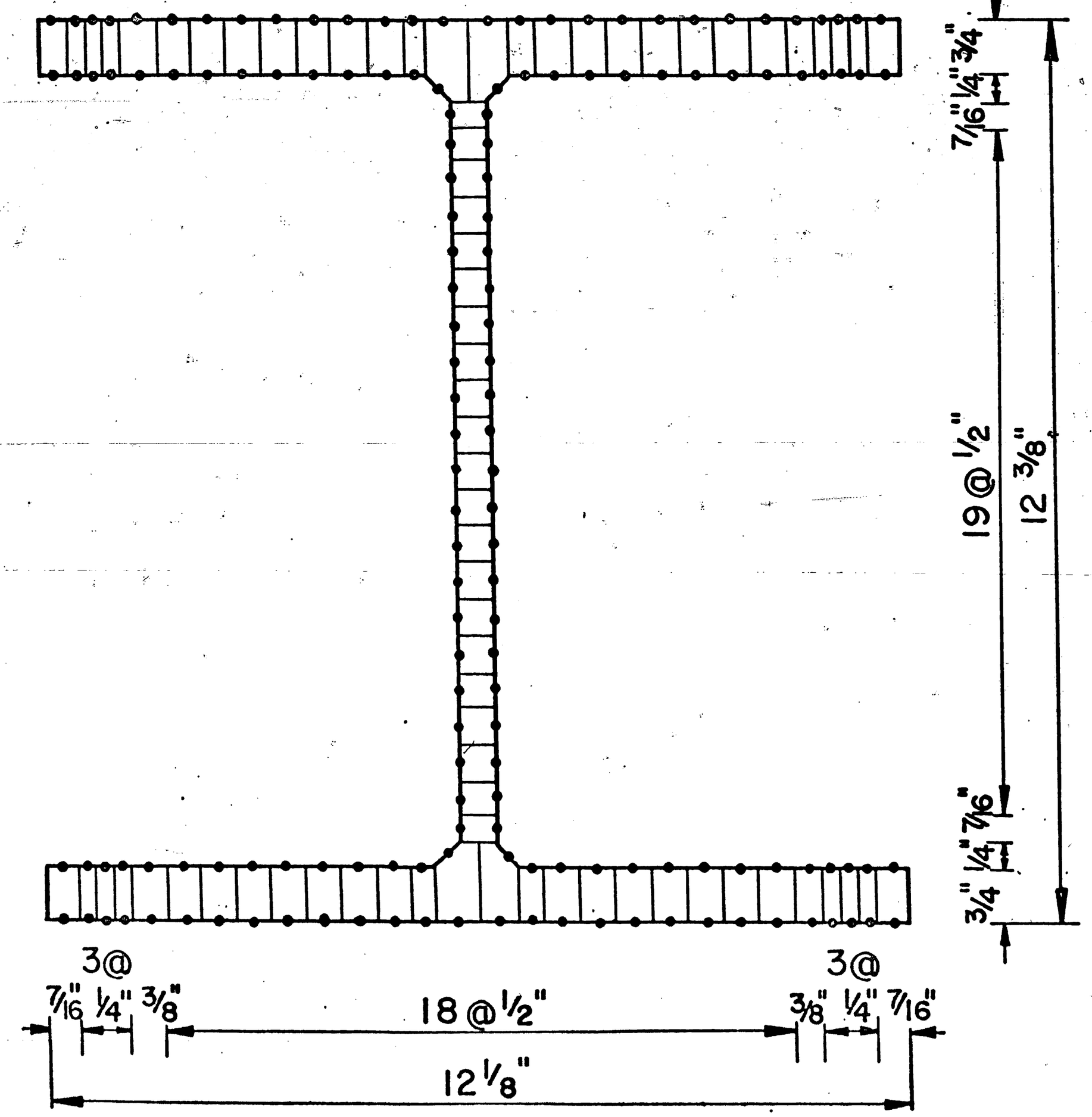

Fig. 6 Sectioning Details for 12H79 Shapes

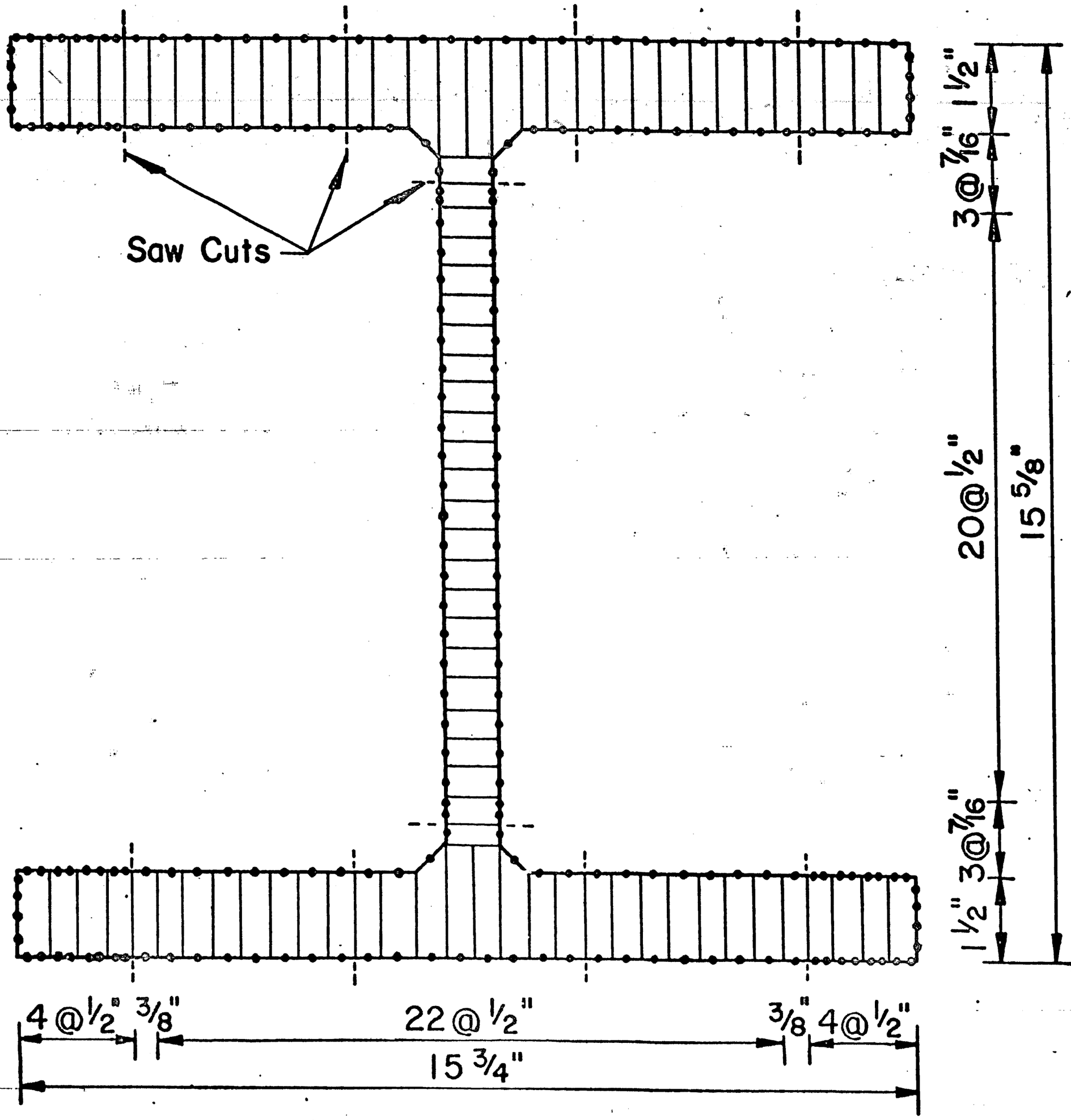

Fig. 7 Sectioning Details for 14H202 Shapes

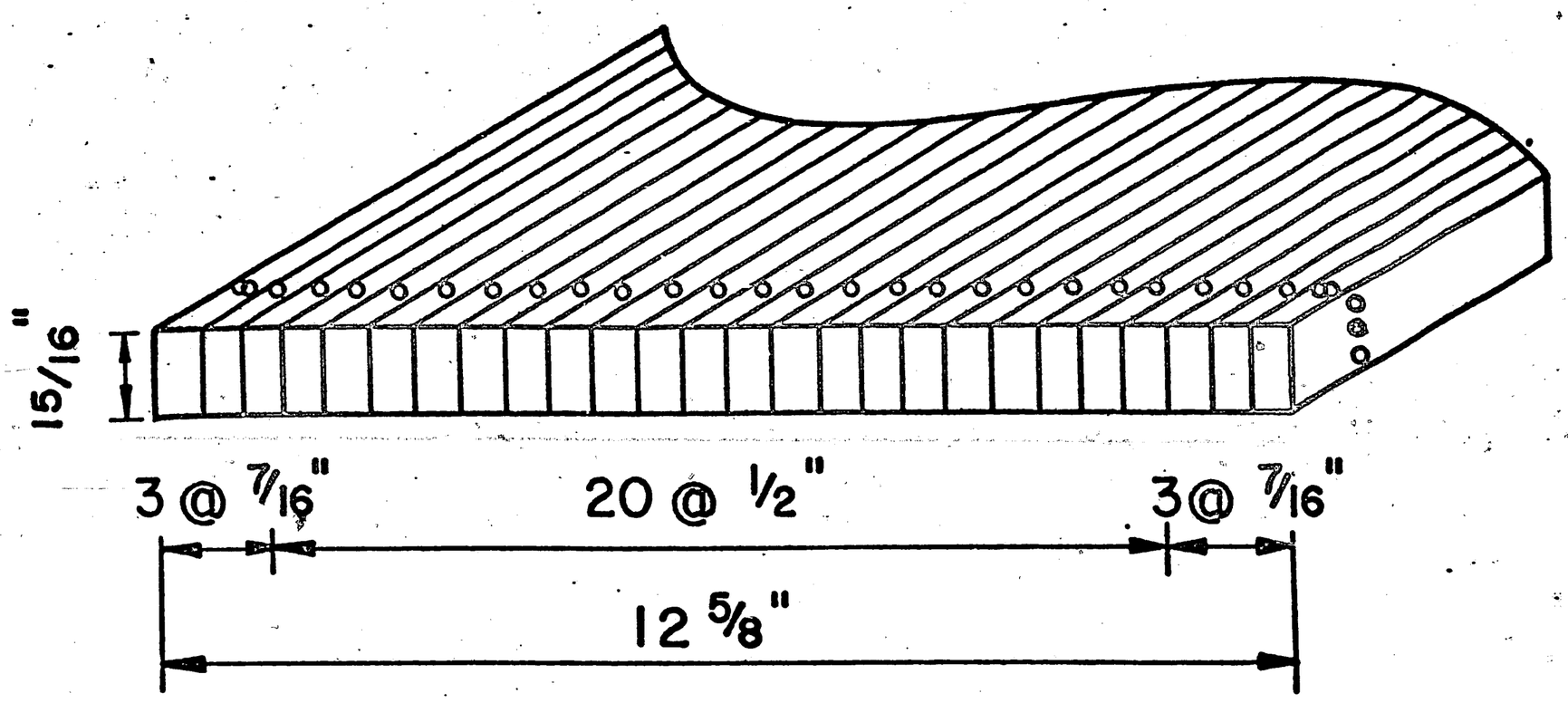

(a) Web Plate (4D)

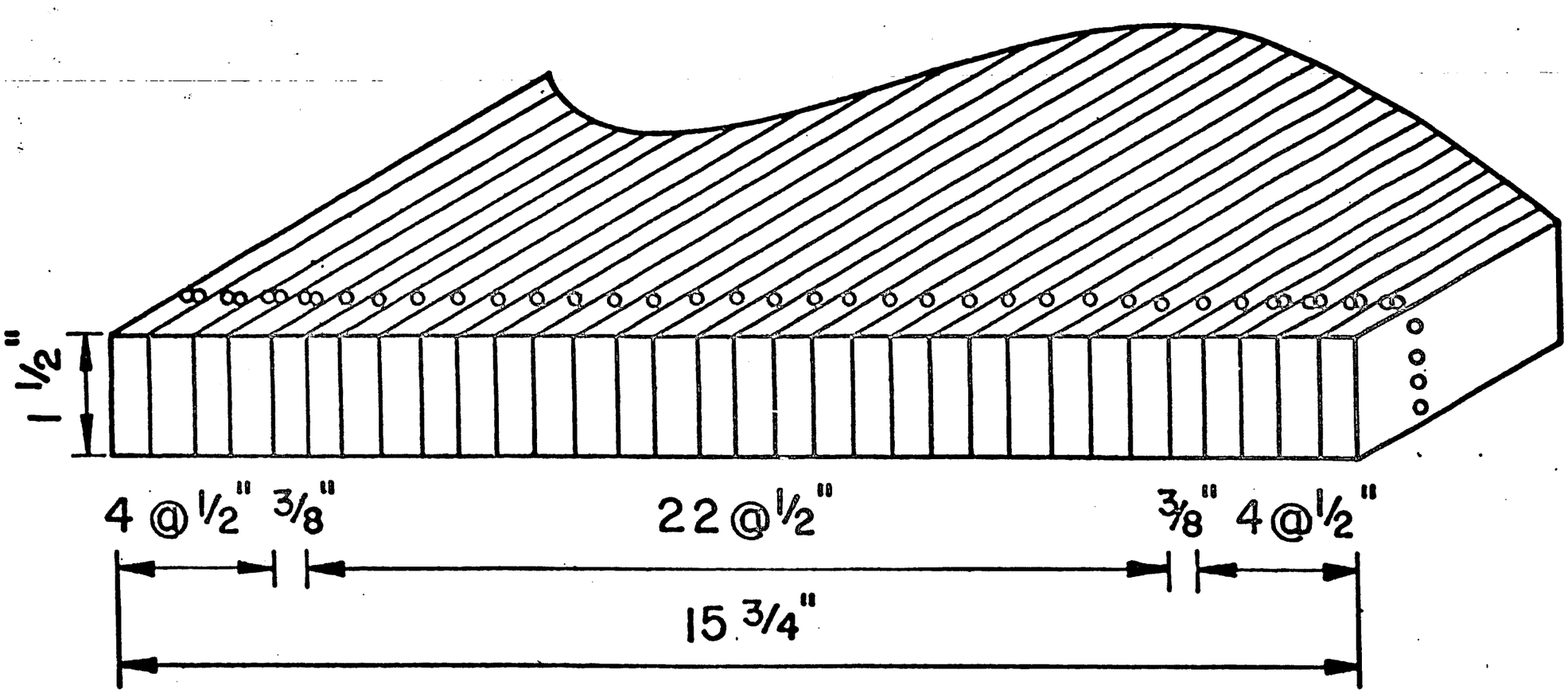

(b) Flange Plates (4E and 4F)

Fig. 8 Sectioning Details for Plates

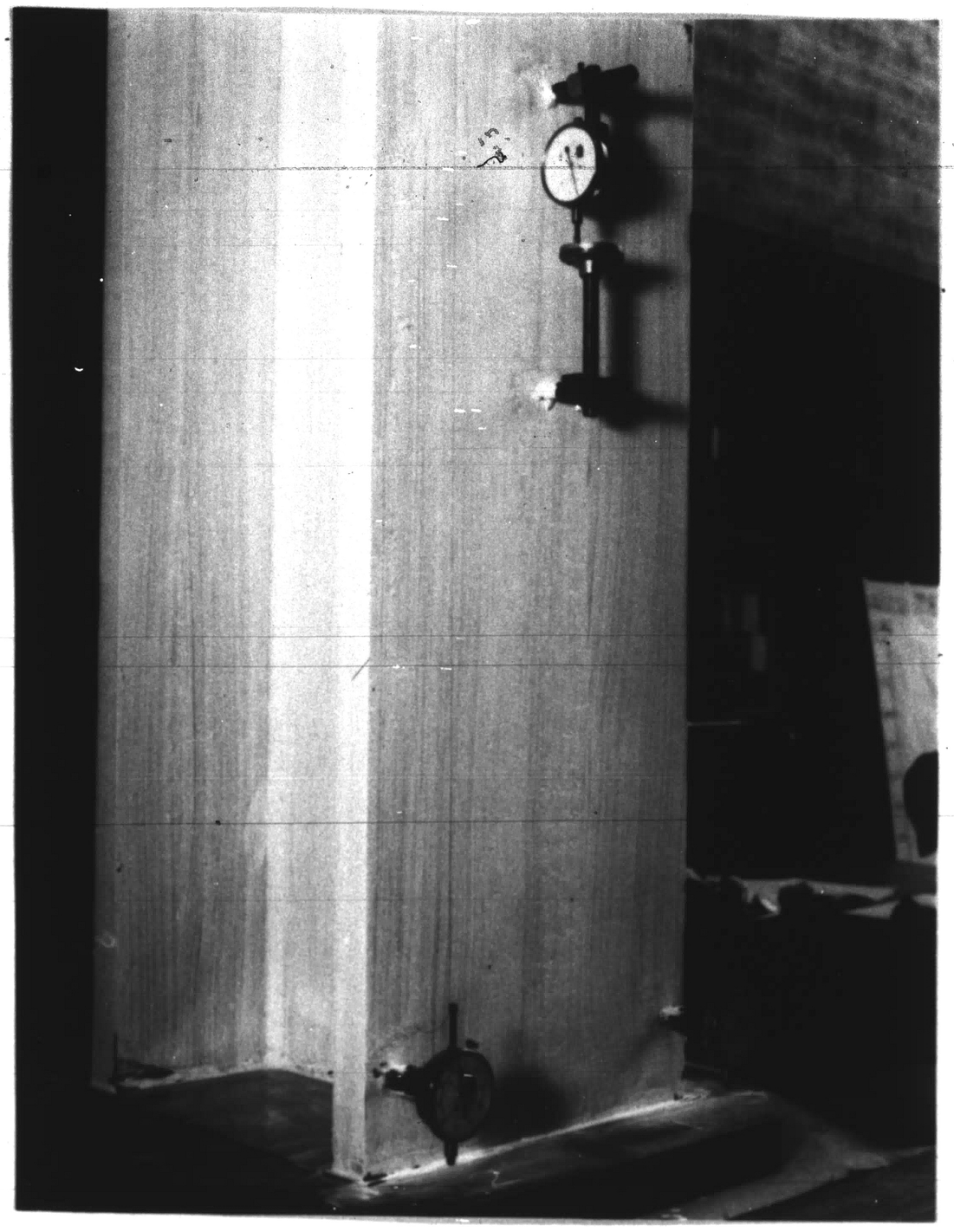

Fig. 9 Stub Column Test Set-Up

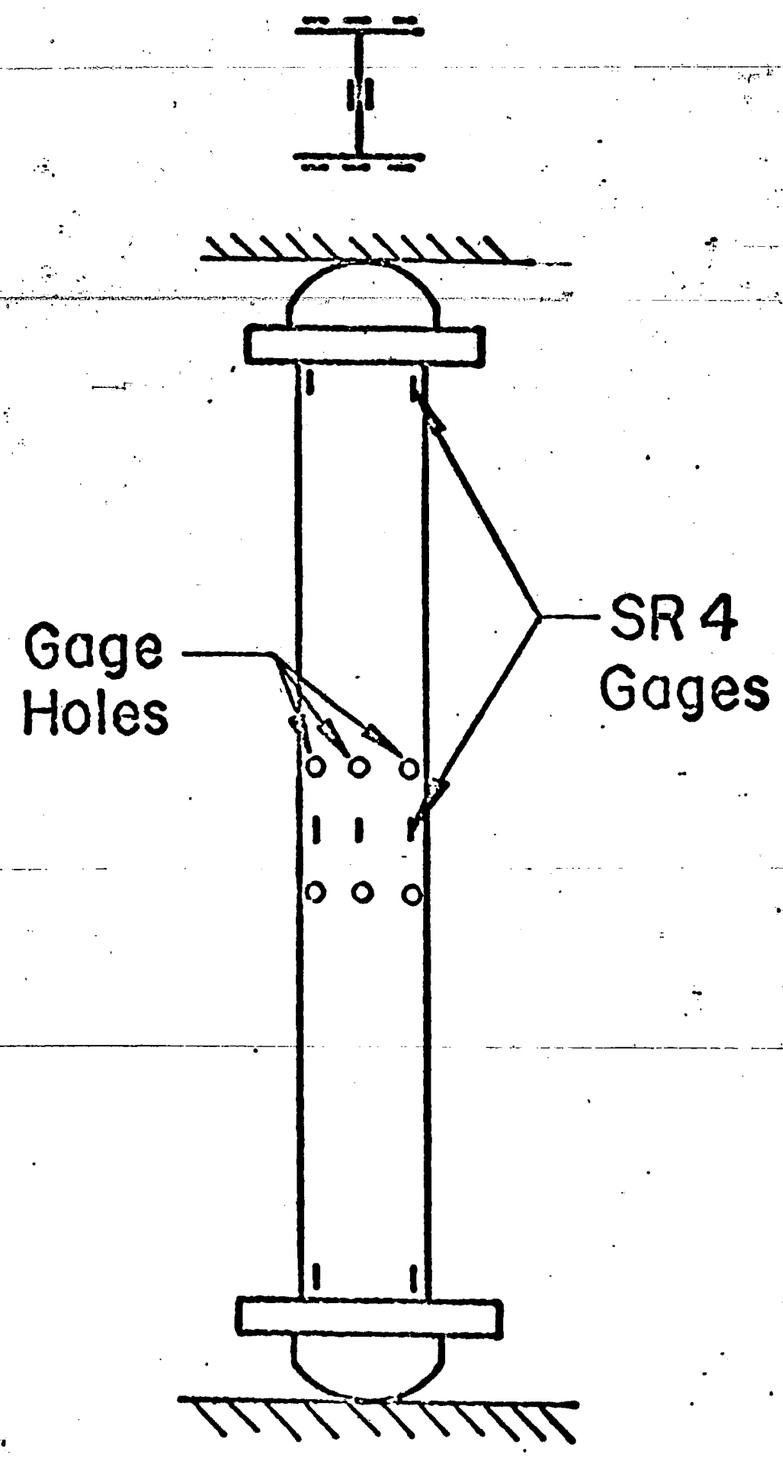

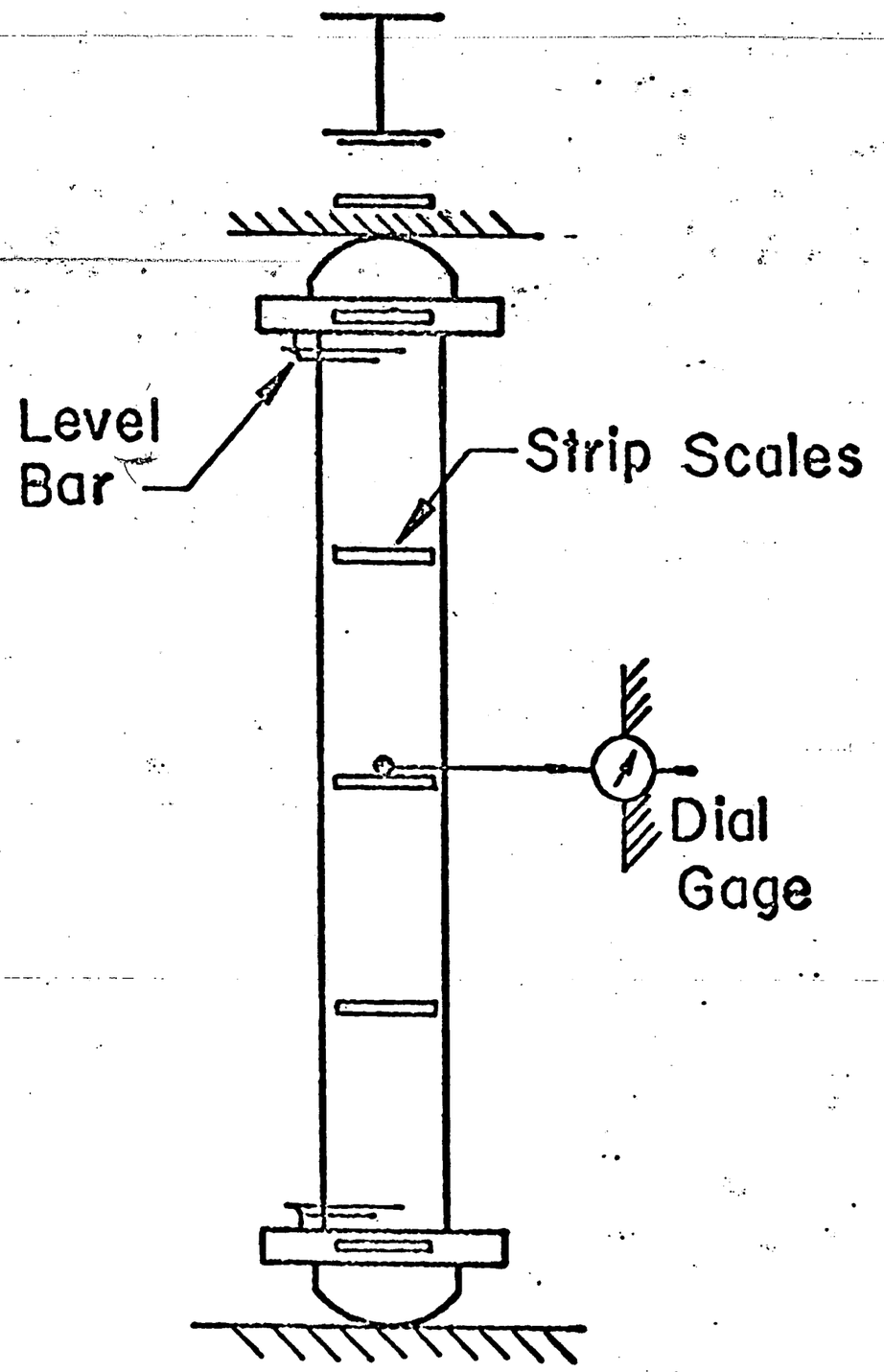

Fig. 10 Pinned-End Column Instrumentation

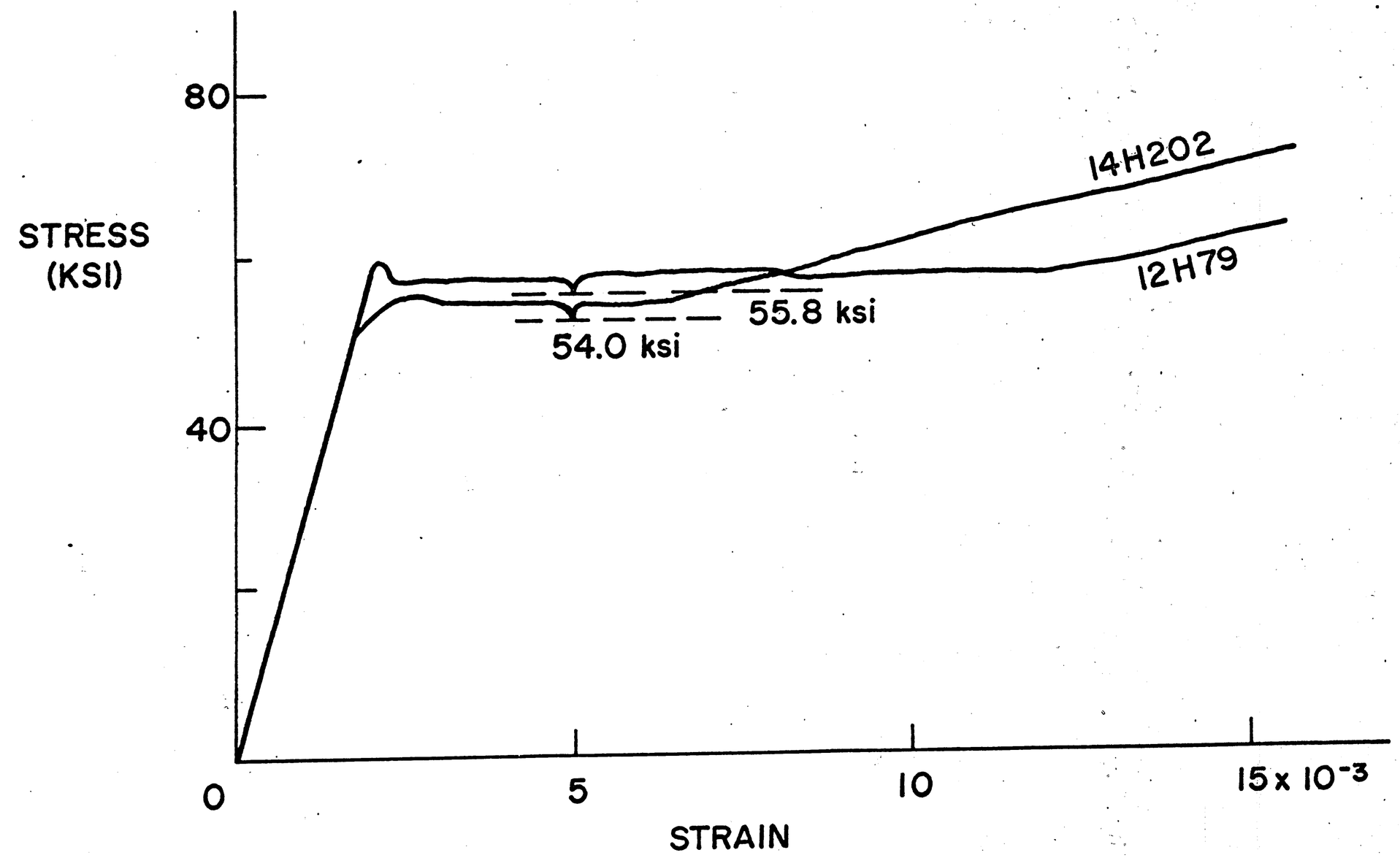

Fig. 11 Average Stress-Strain Curves Obtained from Tension Specimen Tests -- A572(Grade 50) Steel

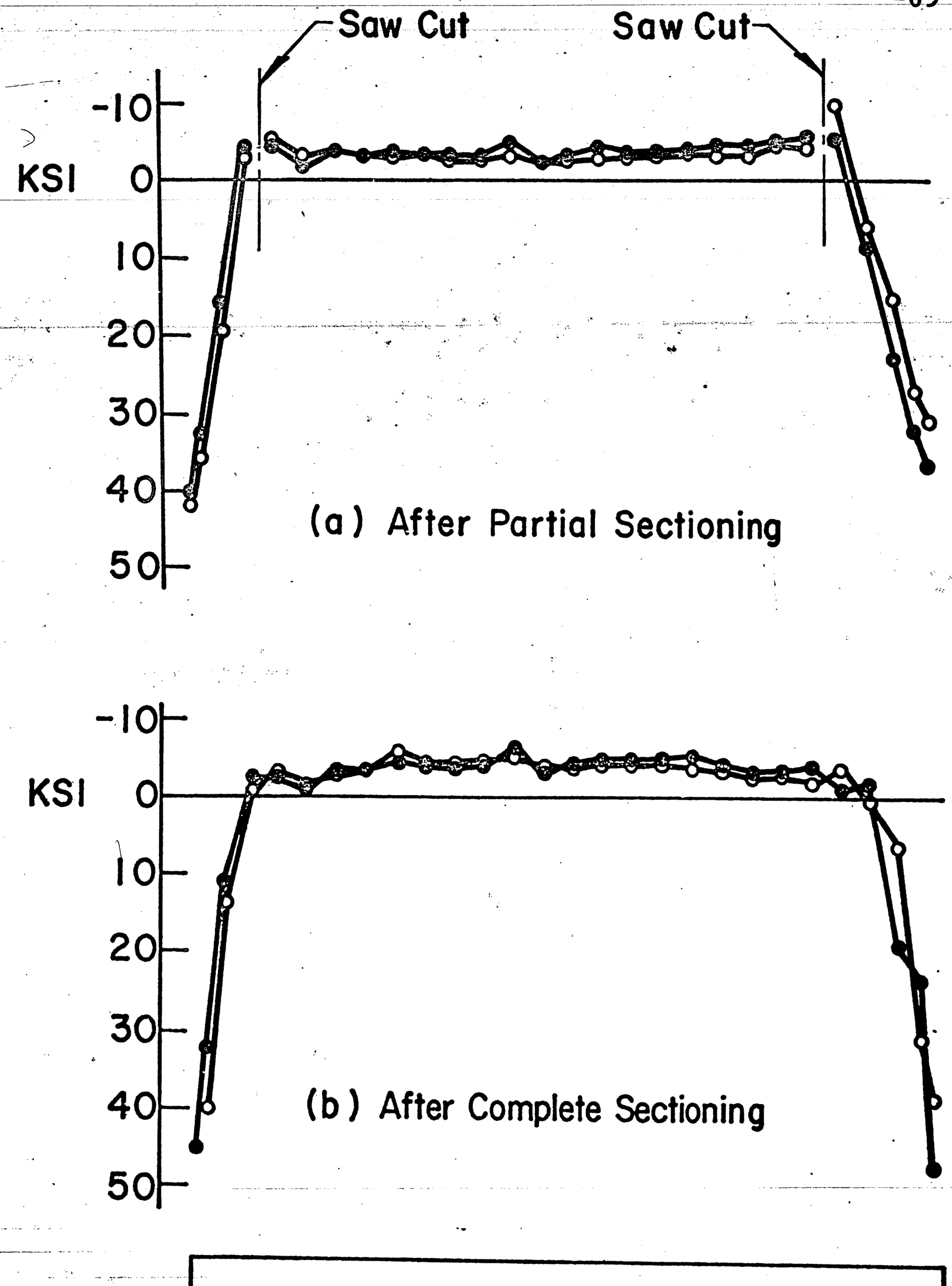

Fig. 12 Residual Stress Distribution in Web Plate: 4D

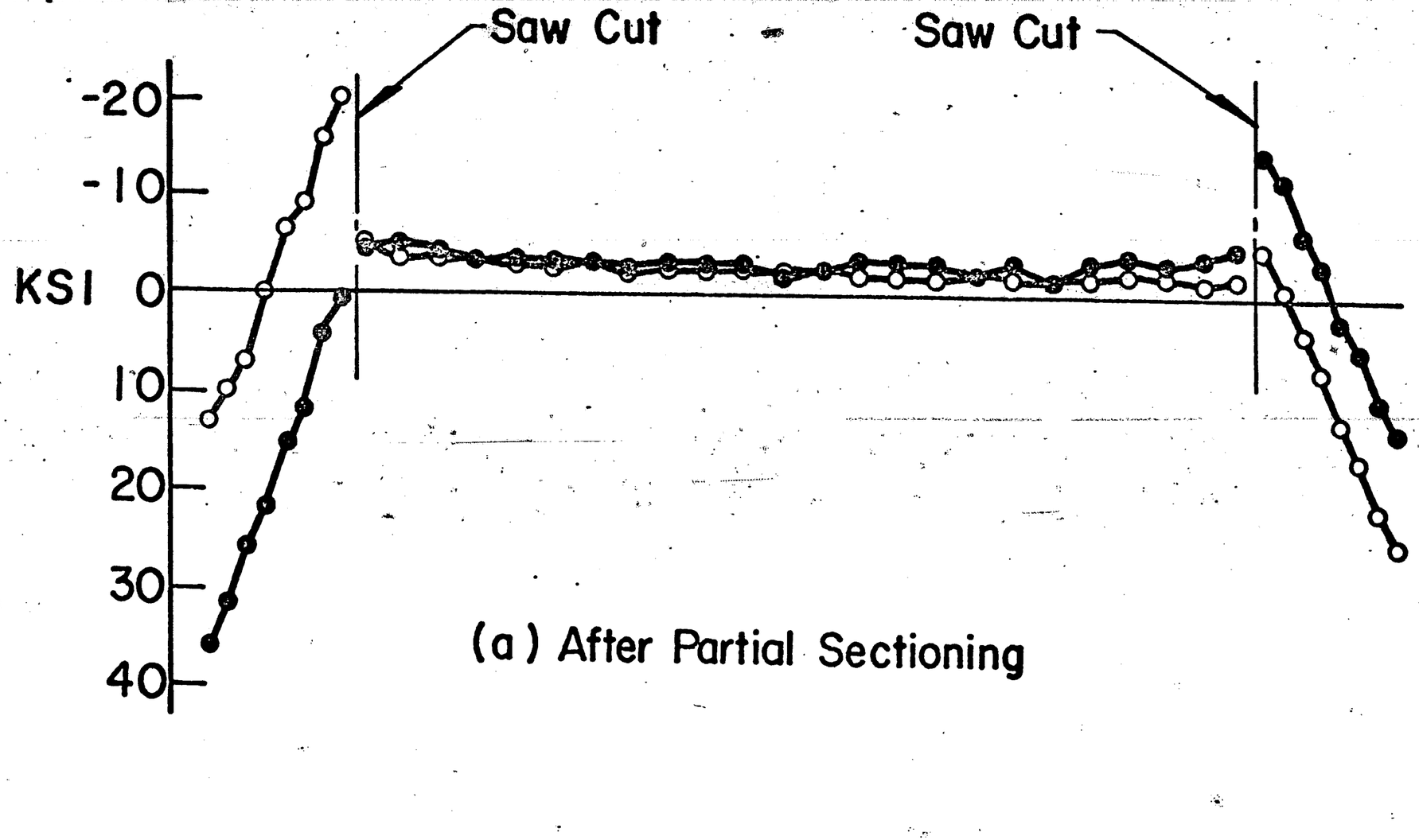

(a) After Partial Sectioning

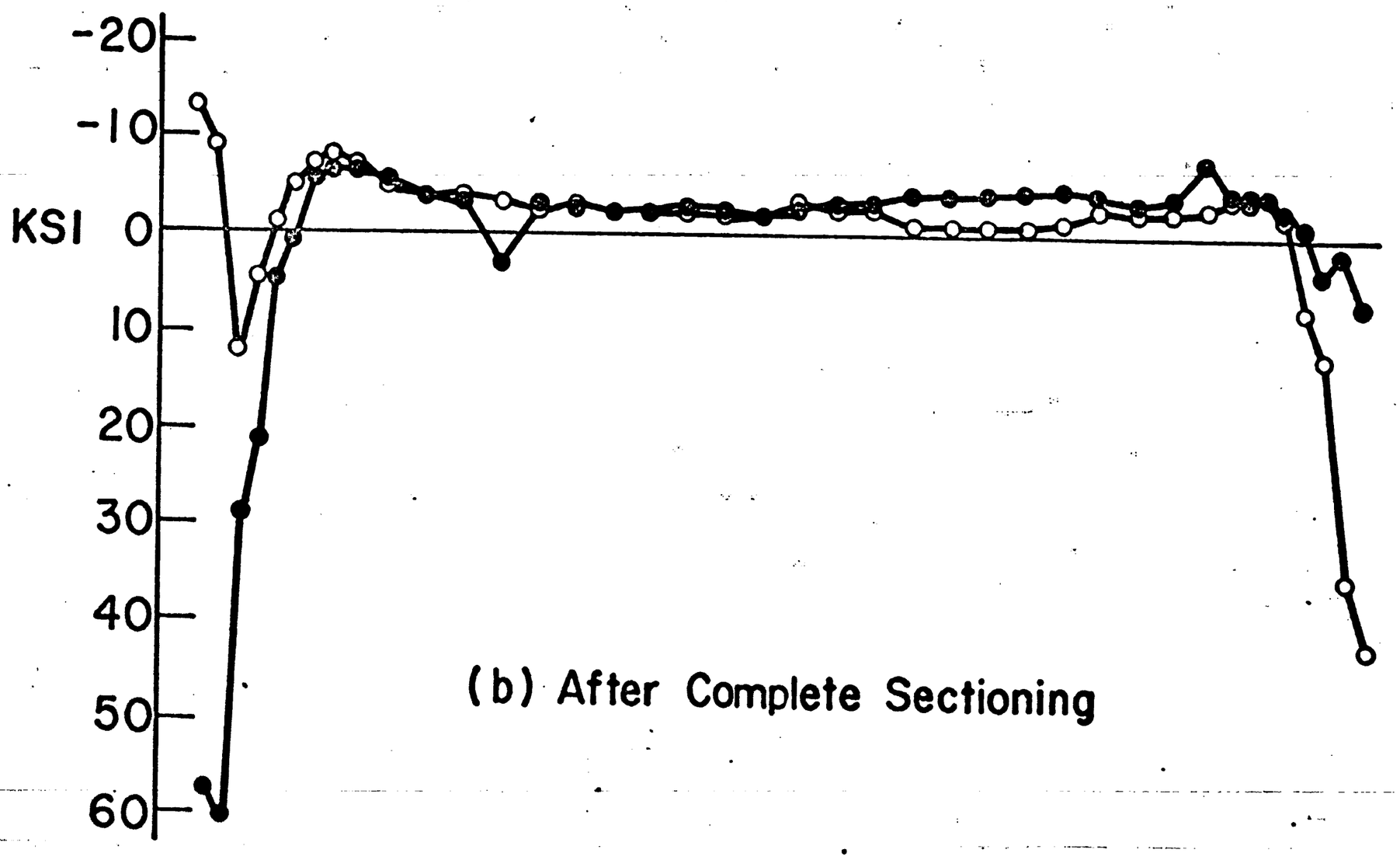

(b) After Complete Sectioning

Plate 15 3/4" x 1 1/2" (FC), A572 (50)

Fig. 13 Residual Stress Distribution in Flange Plate: 4E

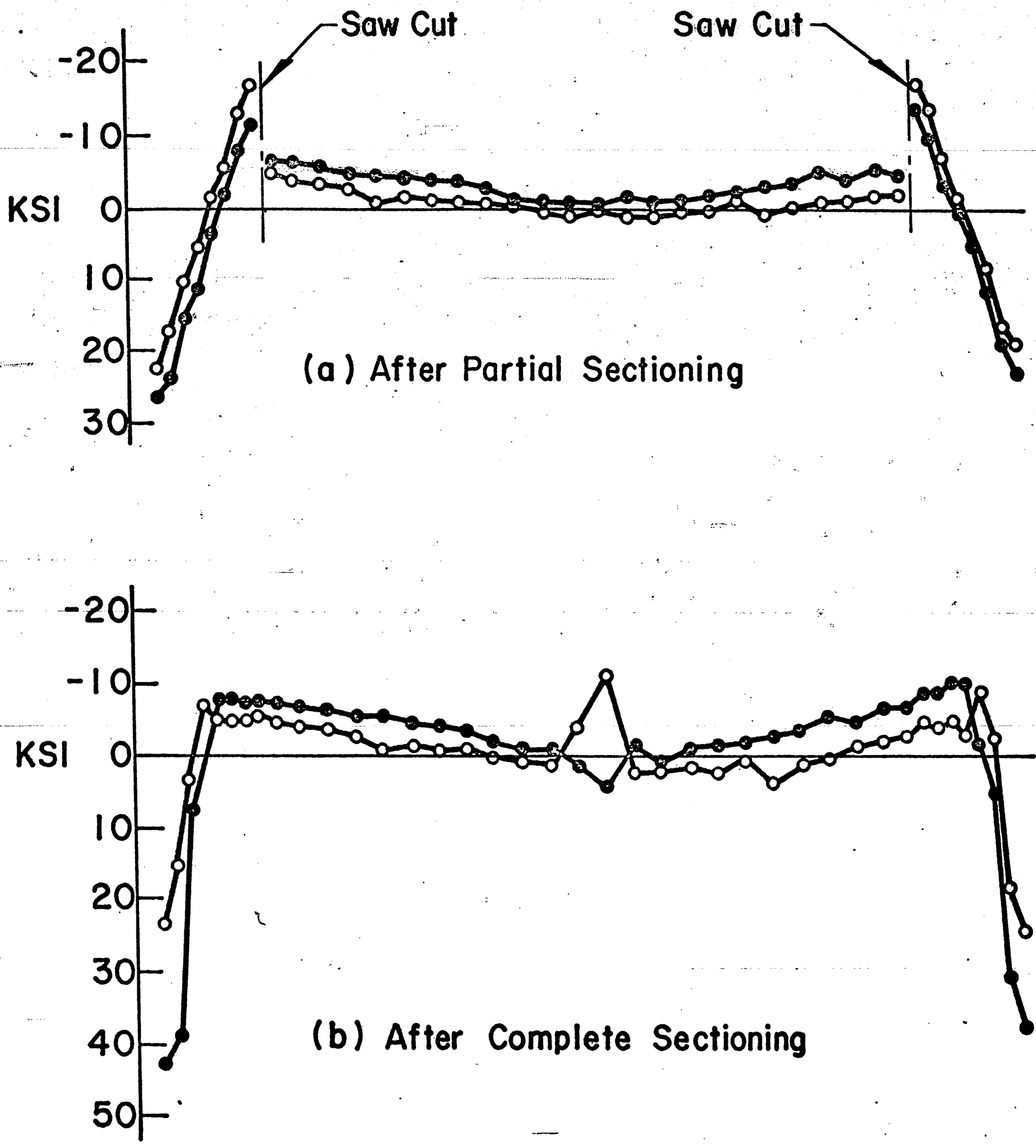

Plate 15 3/4" x 1 1/2" (FC), A572 (50)

Fig. 14 Residual Stress Distribution in Flange Plate: 4F

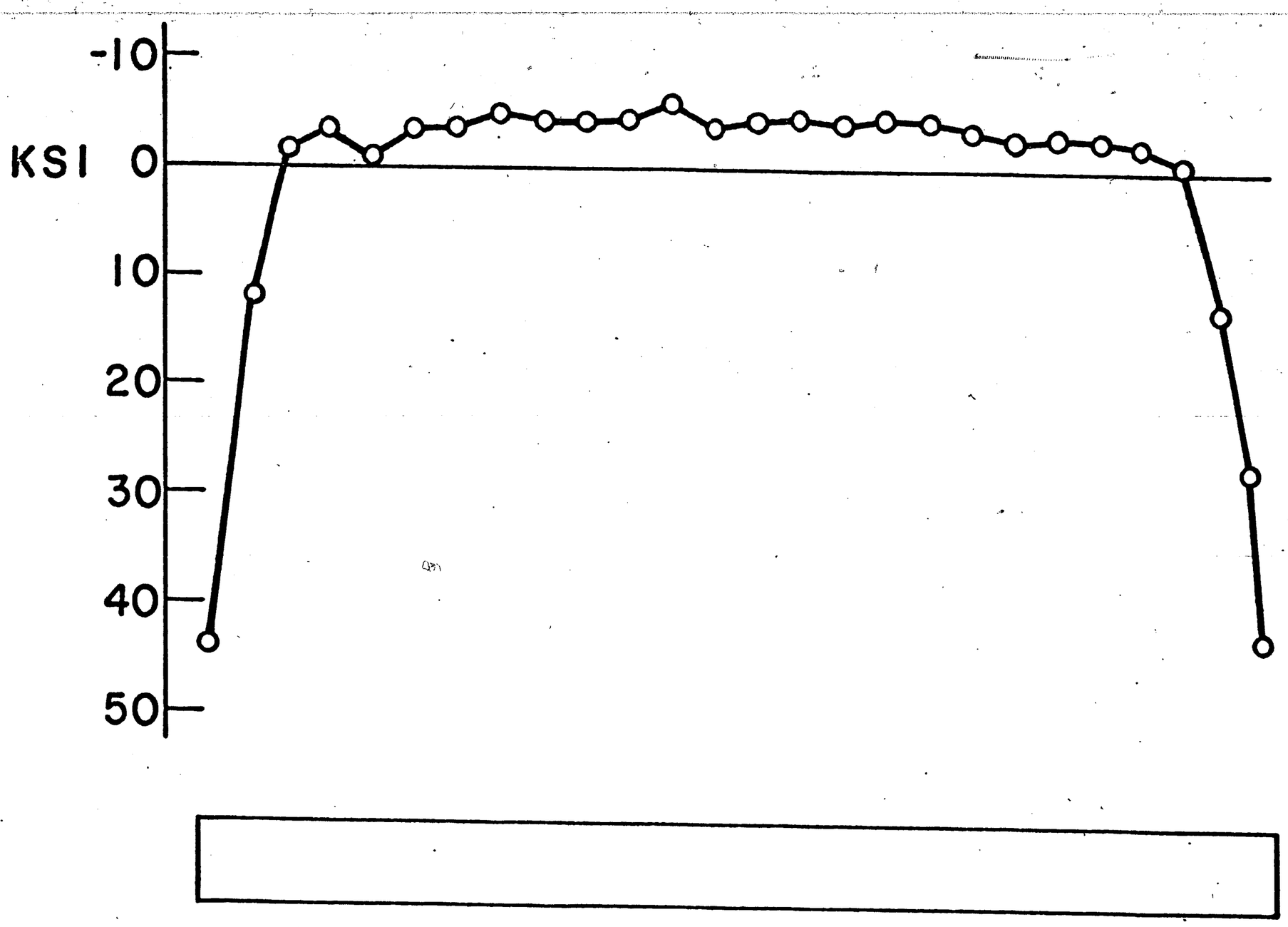

Fig. 15 Average Residual Stress Distribution in Web Plate (4D), A572(50) Steel

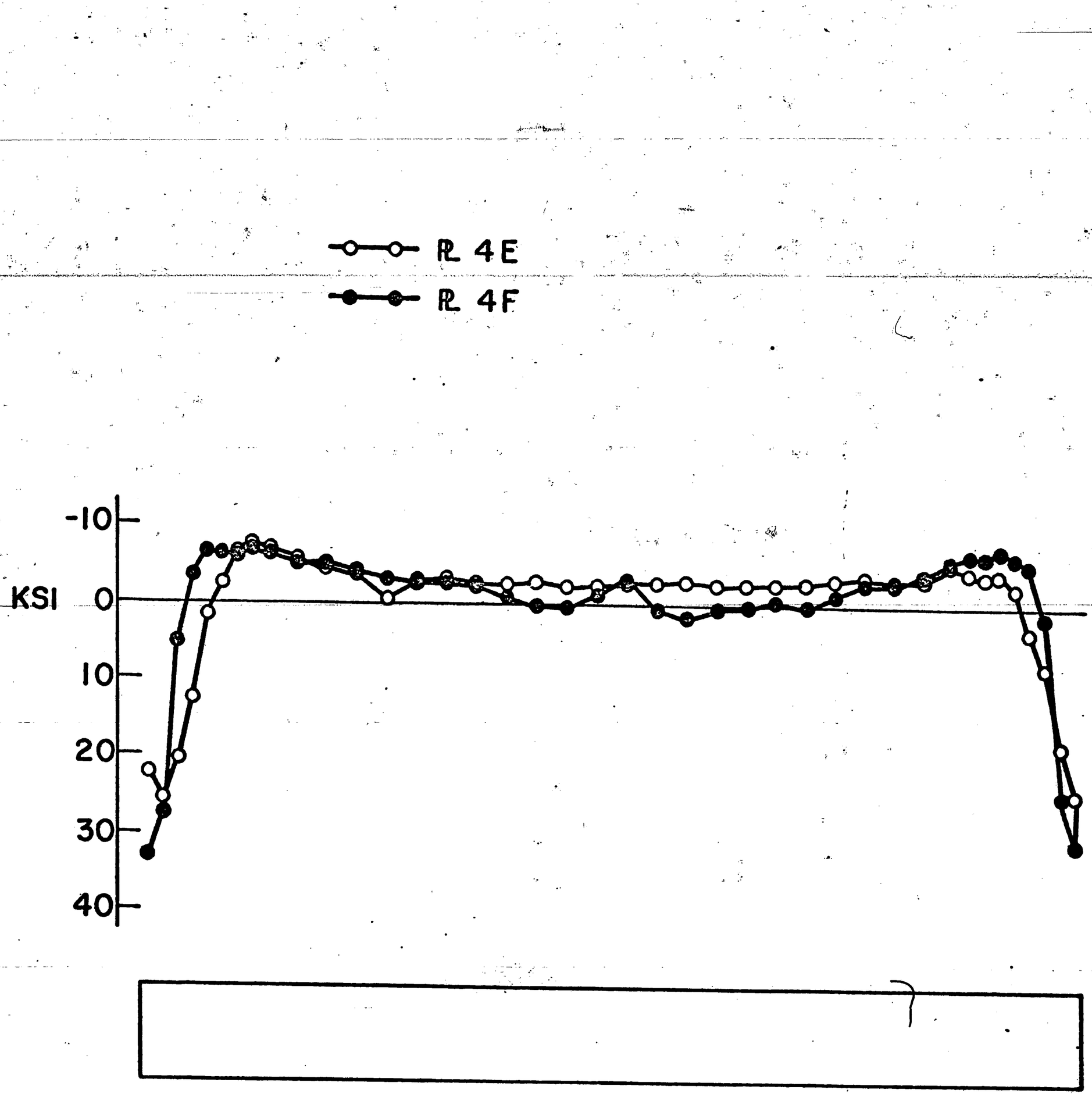

Fig. 16 Average Residual Stress Distribution in Flange Plates (4E and 4F), A572(50) Steel

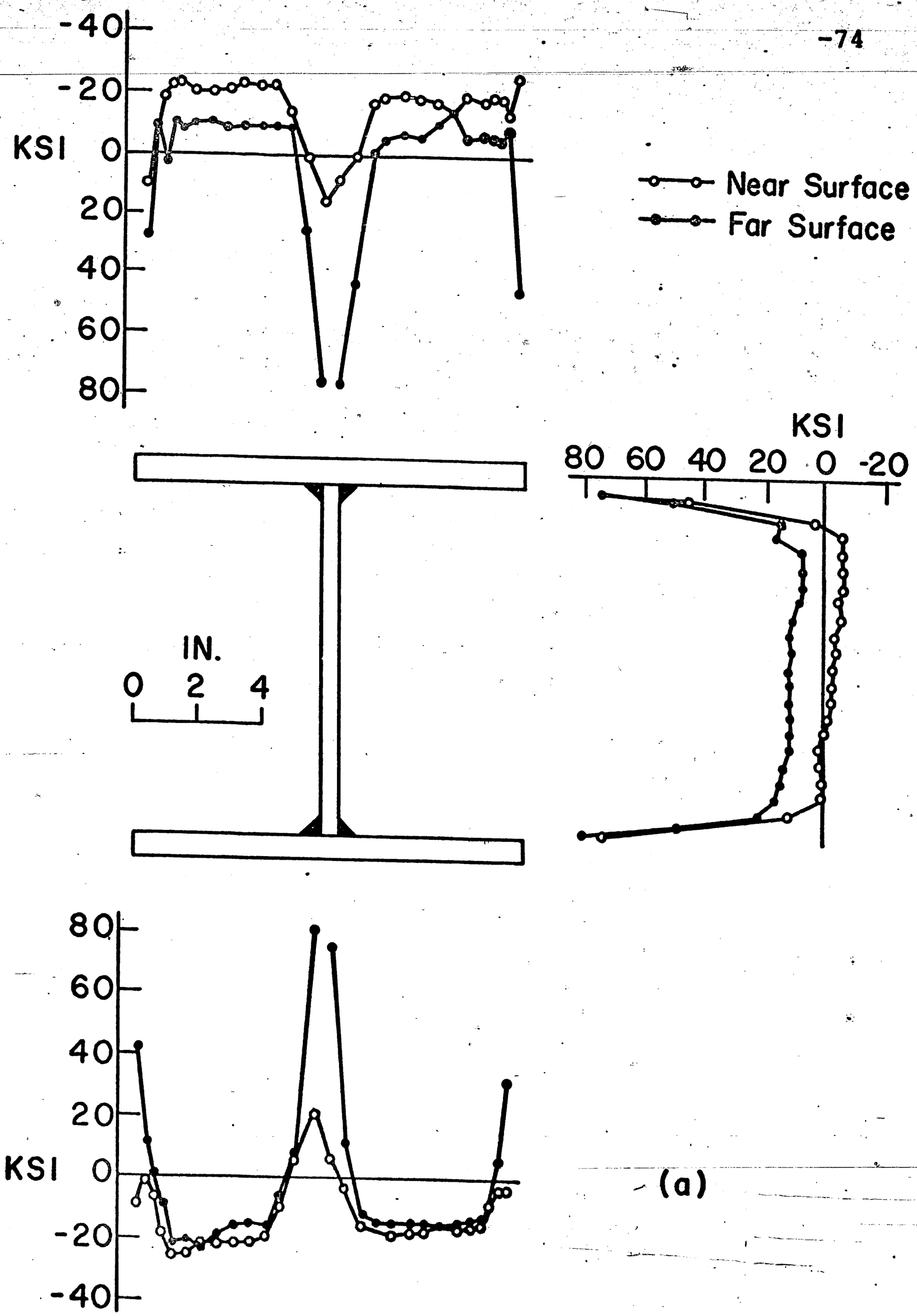

Fig. 17 Residual Stress Distribution in 12H79 (FC) Shape, A572(50) Steel

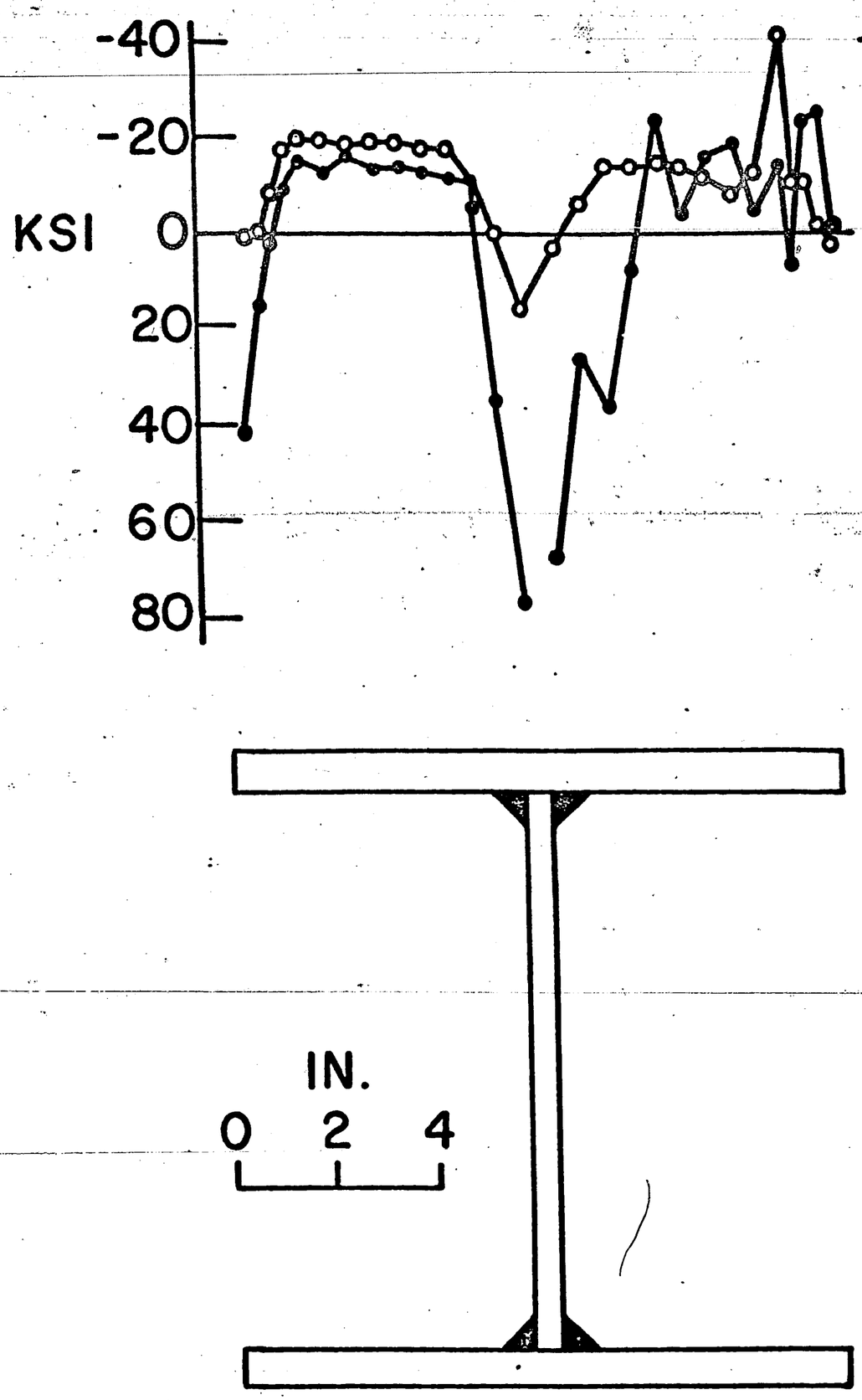

(b)

Fig. 17 Residual Stress Distribution in 12H79 (FC) Shape, A572 (50) Steel (Continued)

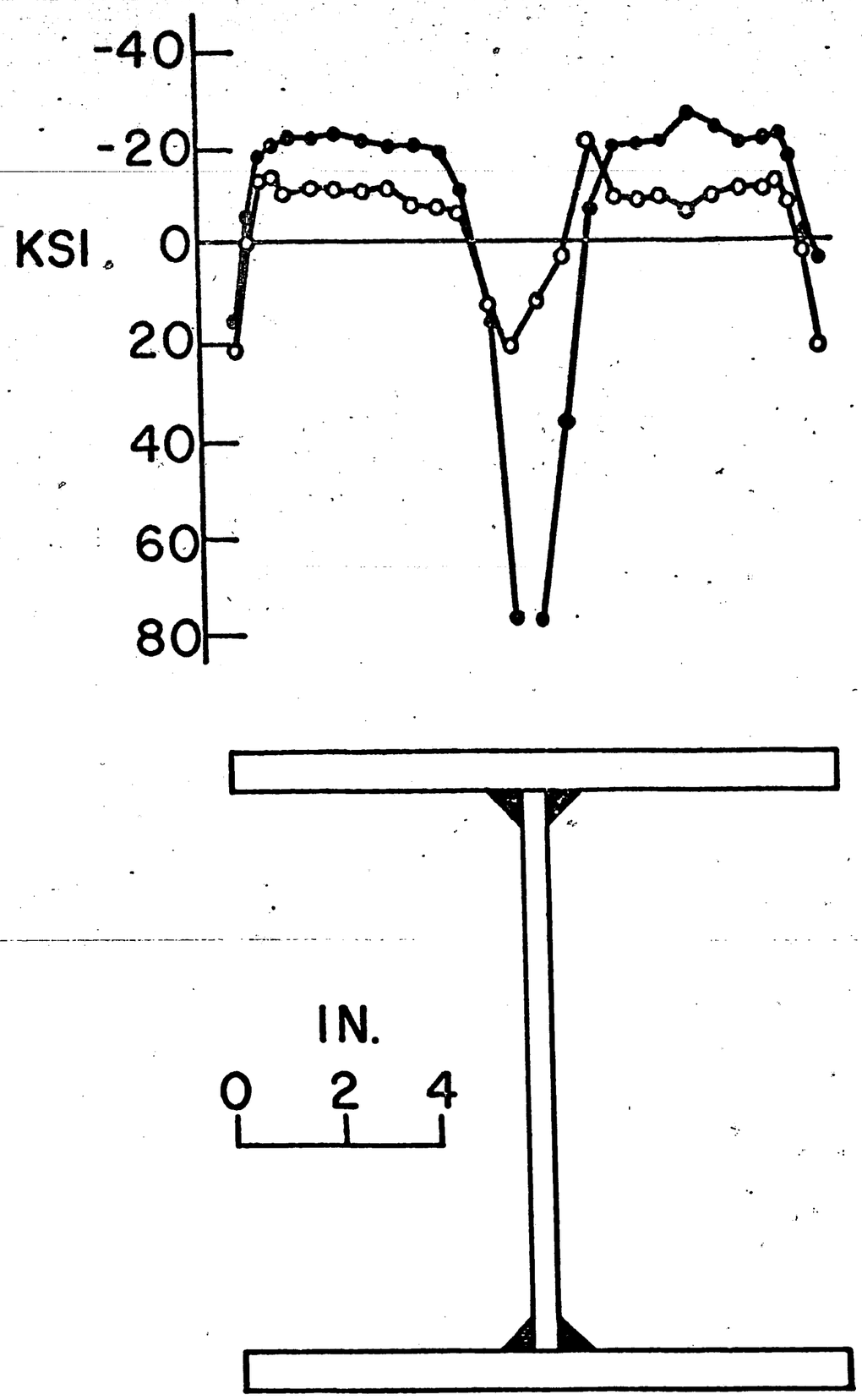

Fig. 17 Residual Stress Distribution in 12H79 (FC) Shape, A572 (50) Steel (Continued)

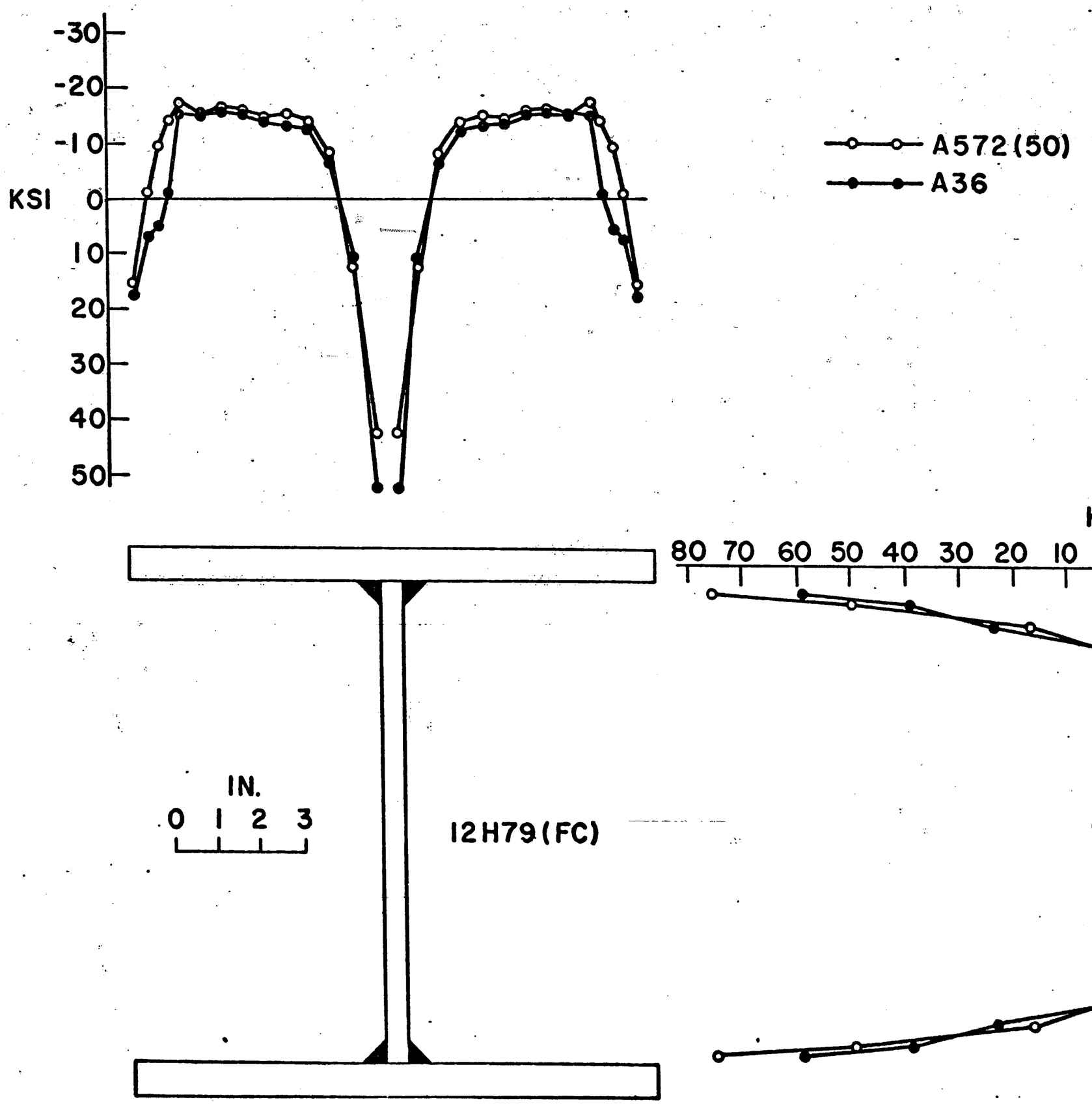

Fig. 18 Average Residual Stress Distribution in 12H79 (FC) Shape

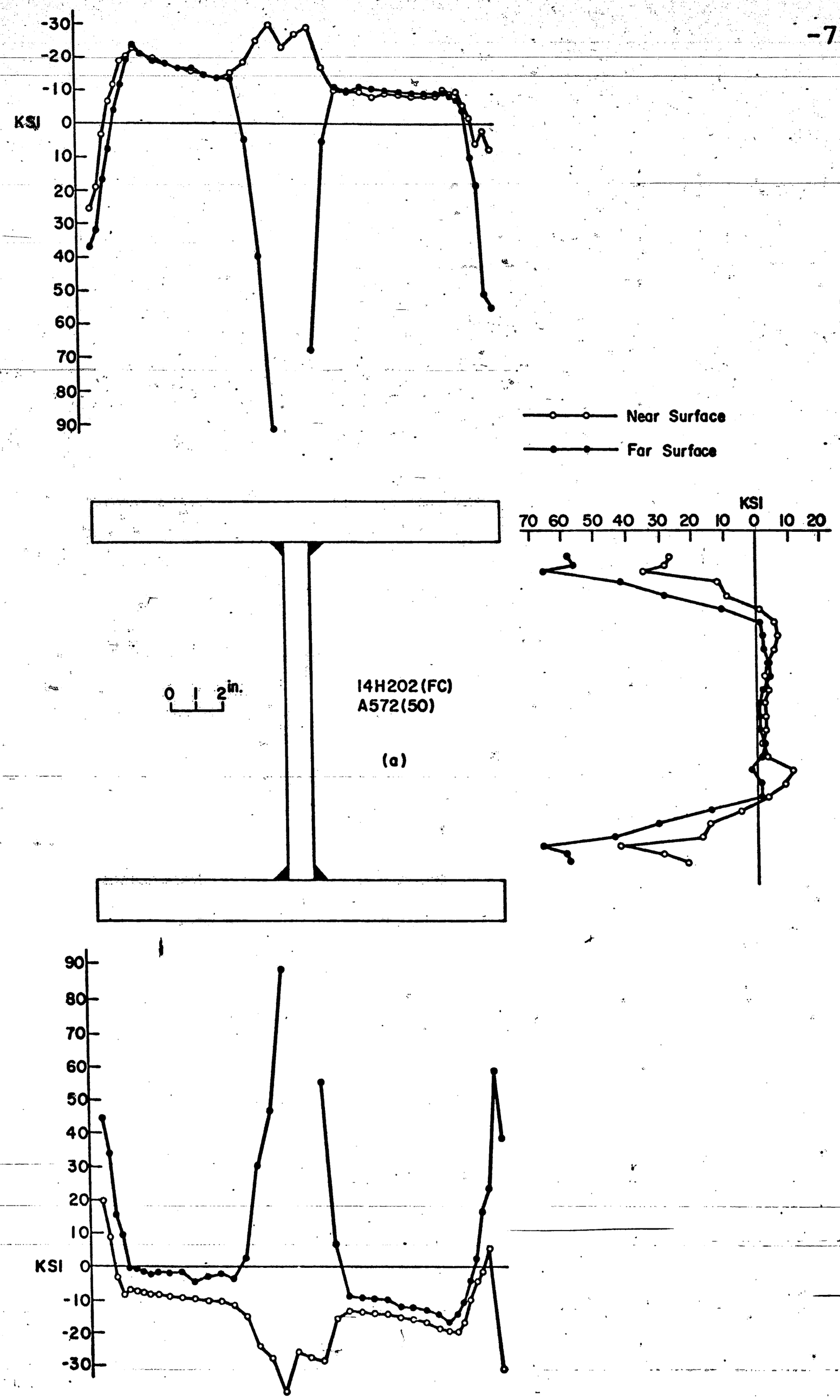

Fig. 19 Residual Stress Distribution in 14H202 (FC) Shape, A572(50) Steel

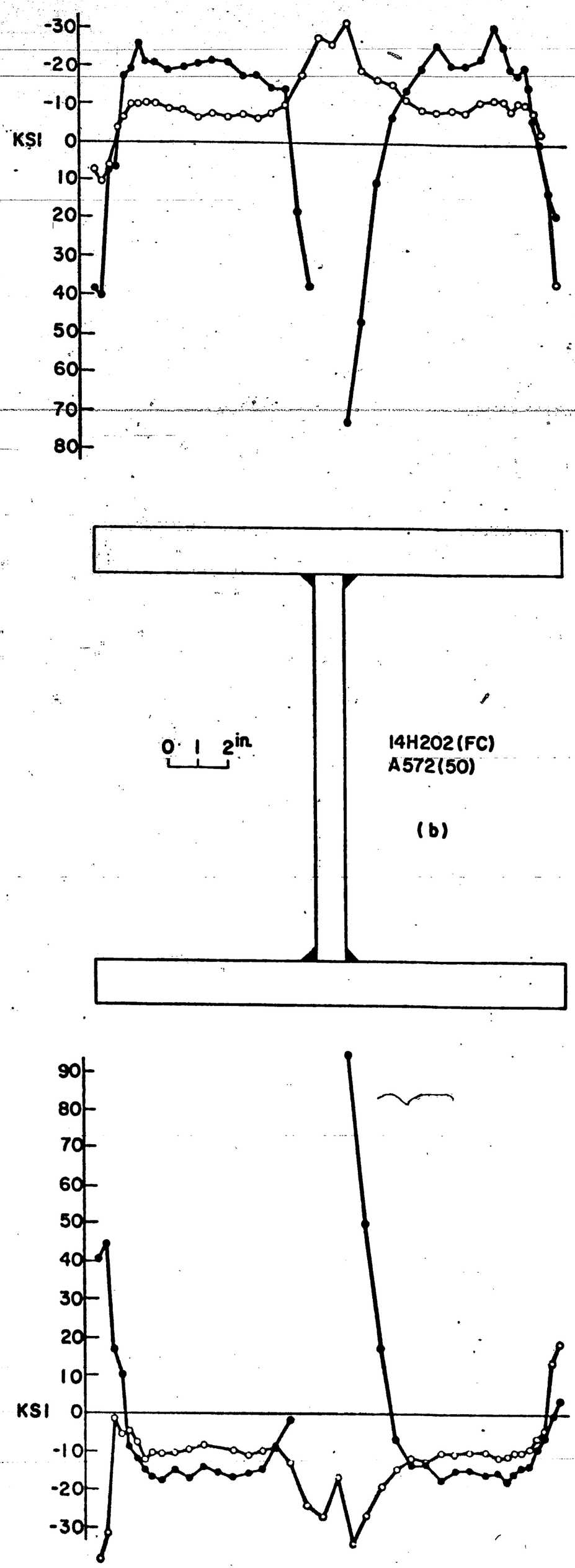

Fig. 19 Residual Stress Distribution in 14H202 (FC) Shape, A572 (50) Steel (Continued)

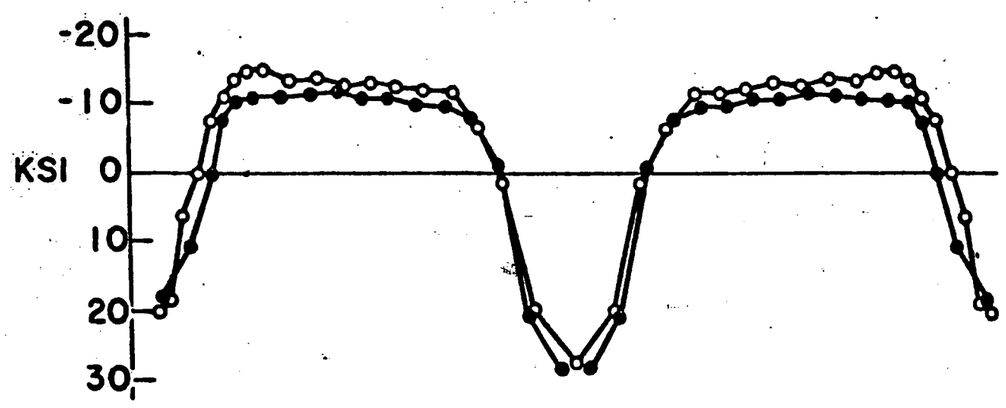

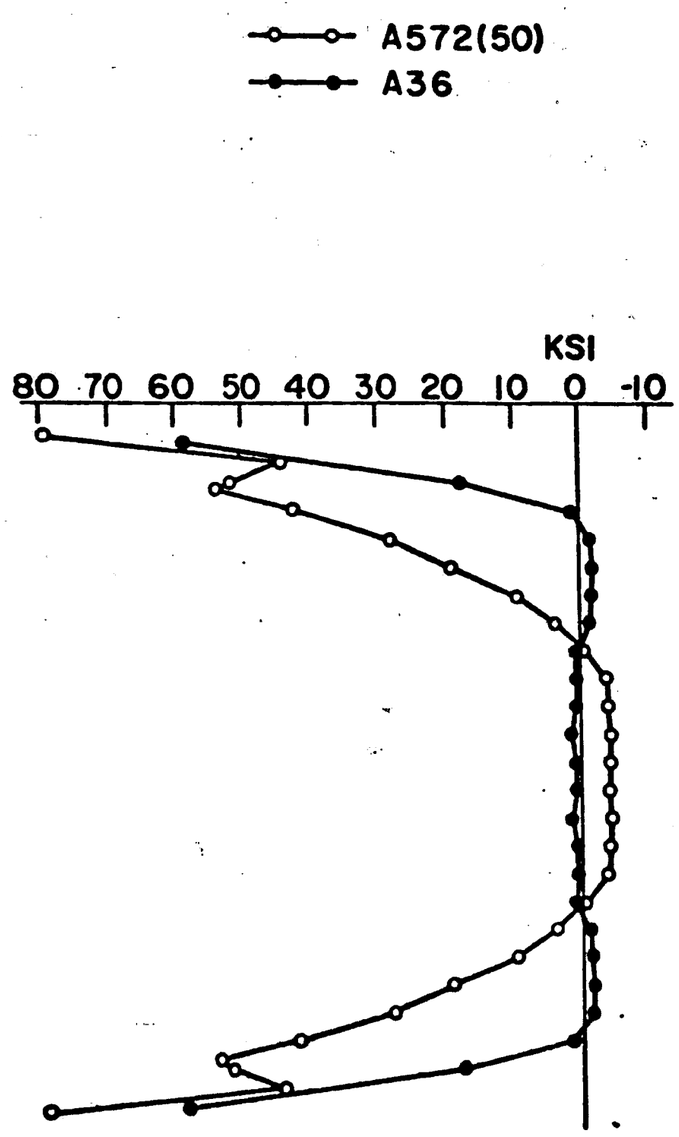

A572(50)
A36

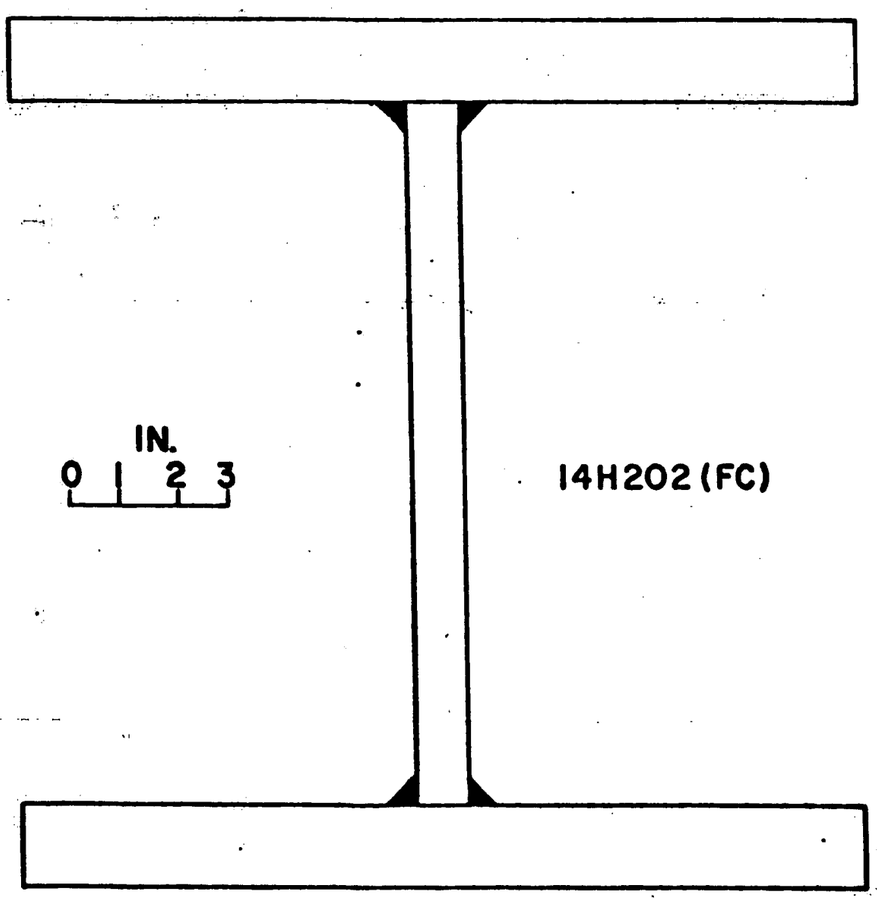

Fig. 20 Average Residual Stress Distribution in 14H202 (FC) Shape

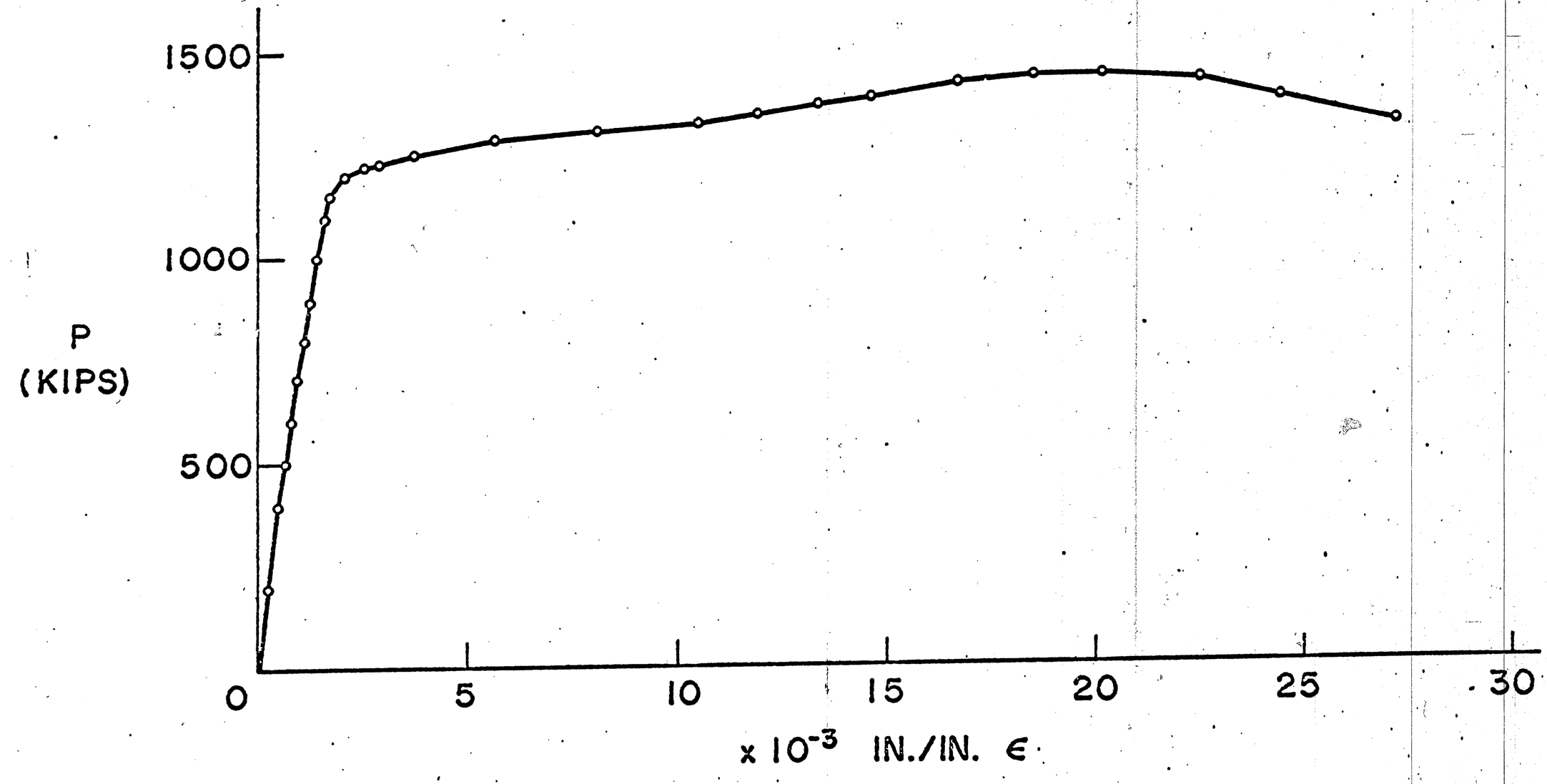

Fig. 21 Stub Column Curve, 12H79(FC), A572(50)

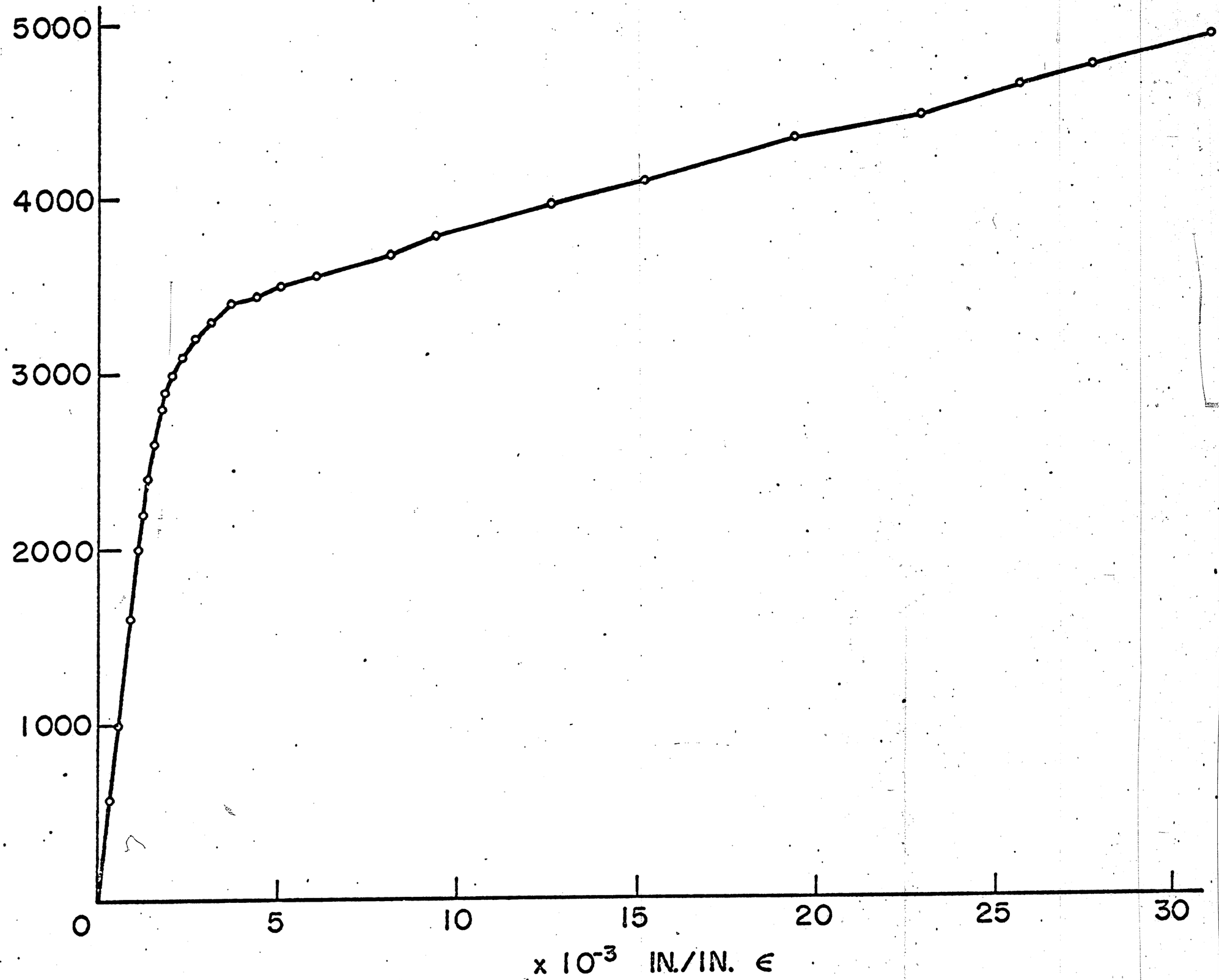

Fig. 22 Stub Column Curve, 14H202(FC), A572(50)

Fig. 23 Deformed Stub Column,
12H79 (FC) Shape

Fig. 24 Deformed Stub Column, 14H202 (FC) Shape

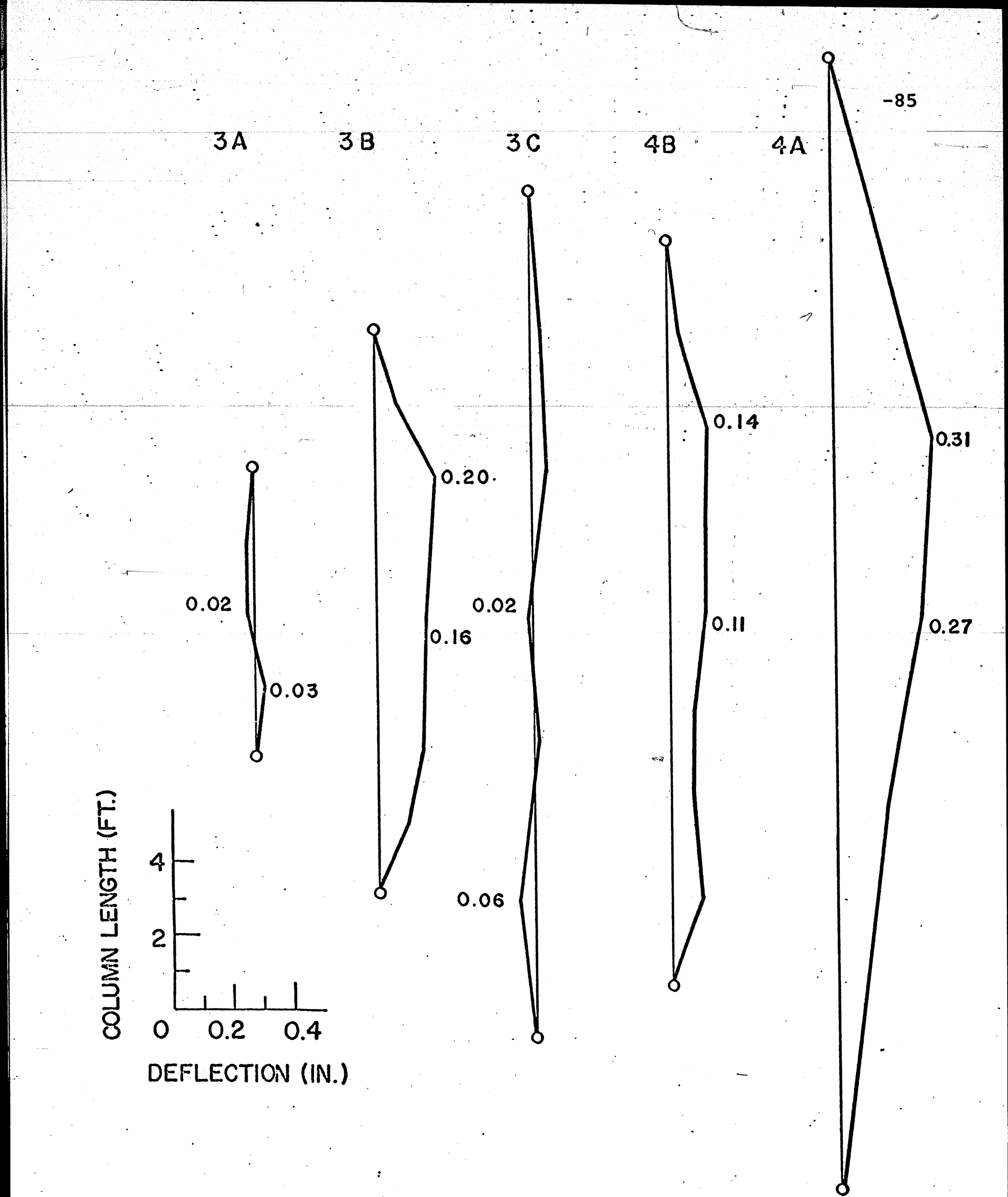

Fig. 25 Initial Out-of-Straightness of Test Columns

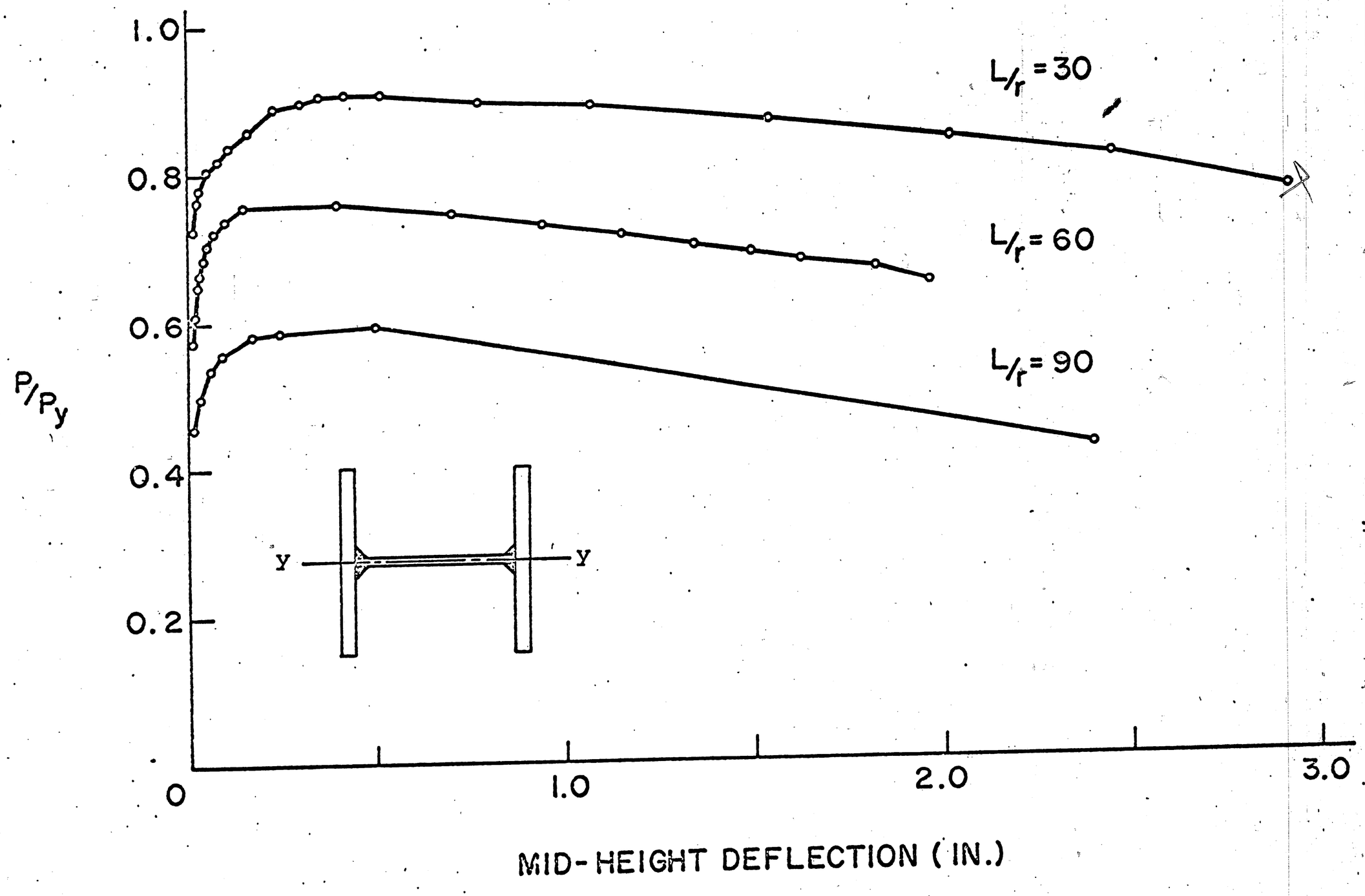

Fig. 26 Load-Deflection Curves of 12H79(FC) Columns

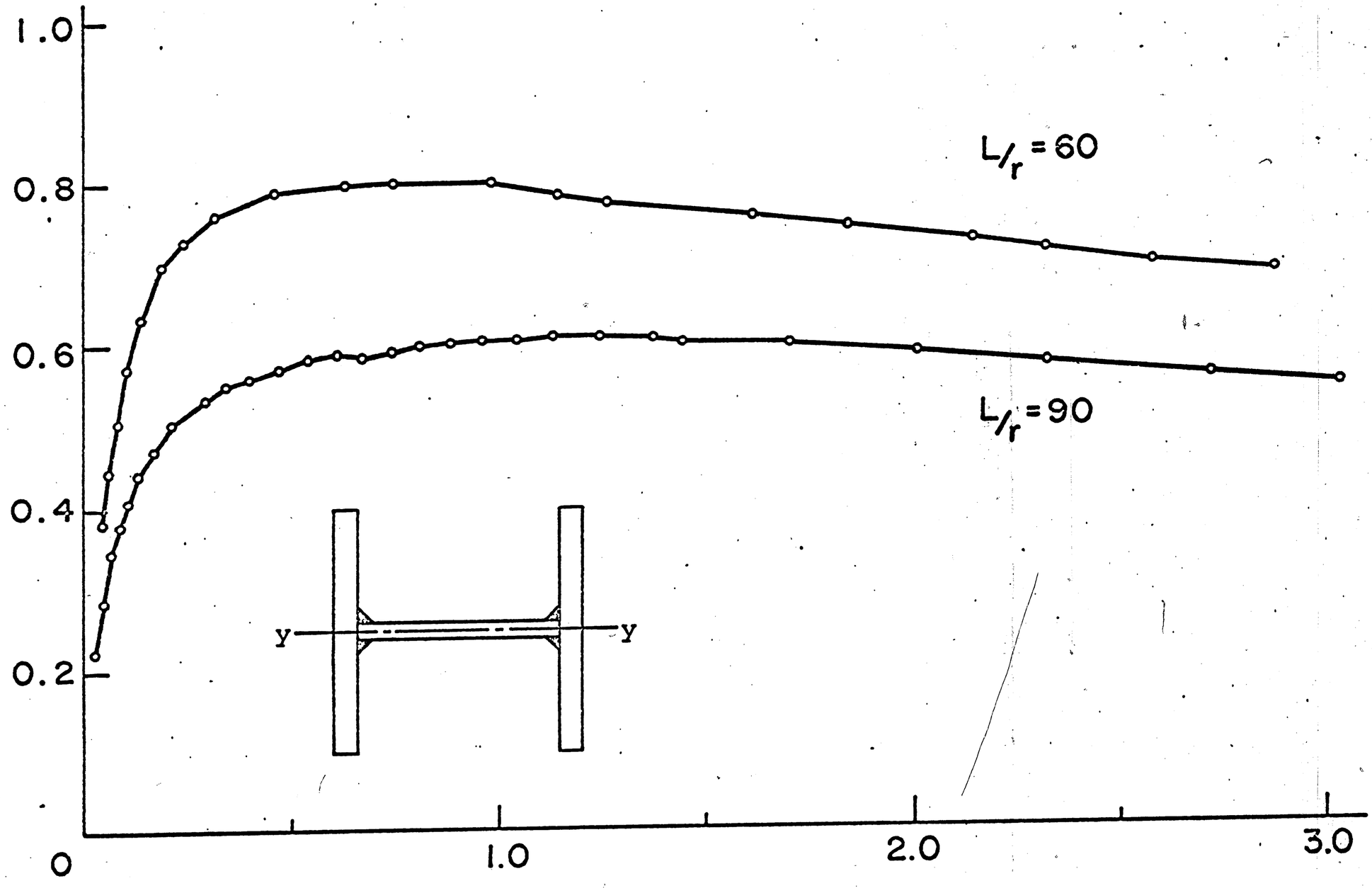

Fig. 27 Load-Deflection Curves of 14H202(FC) Columns

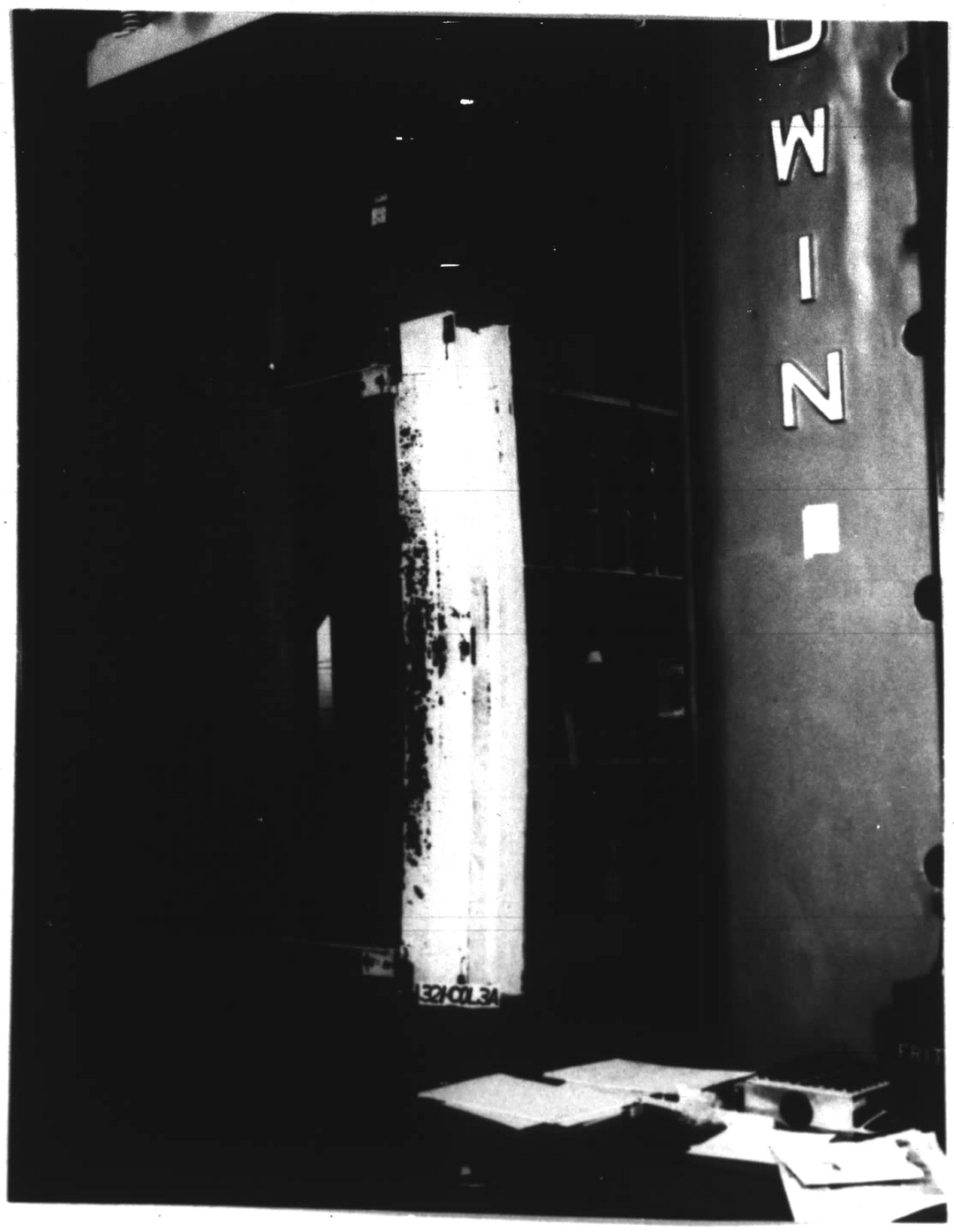

Fig. 28 Deflected Column: 3A, 12H79 (FC), L/r = 30

Fig. 29 Deflected Column: 3B, 12H79 (FC), L/r = 60

Fig. 30 Deflected Column: 3C, 12H79 (FC), L/r = 90

Fig. 31 Deflected Column: 4B, 14H202 (FC), L/r = 60

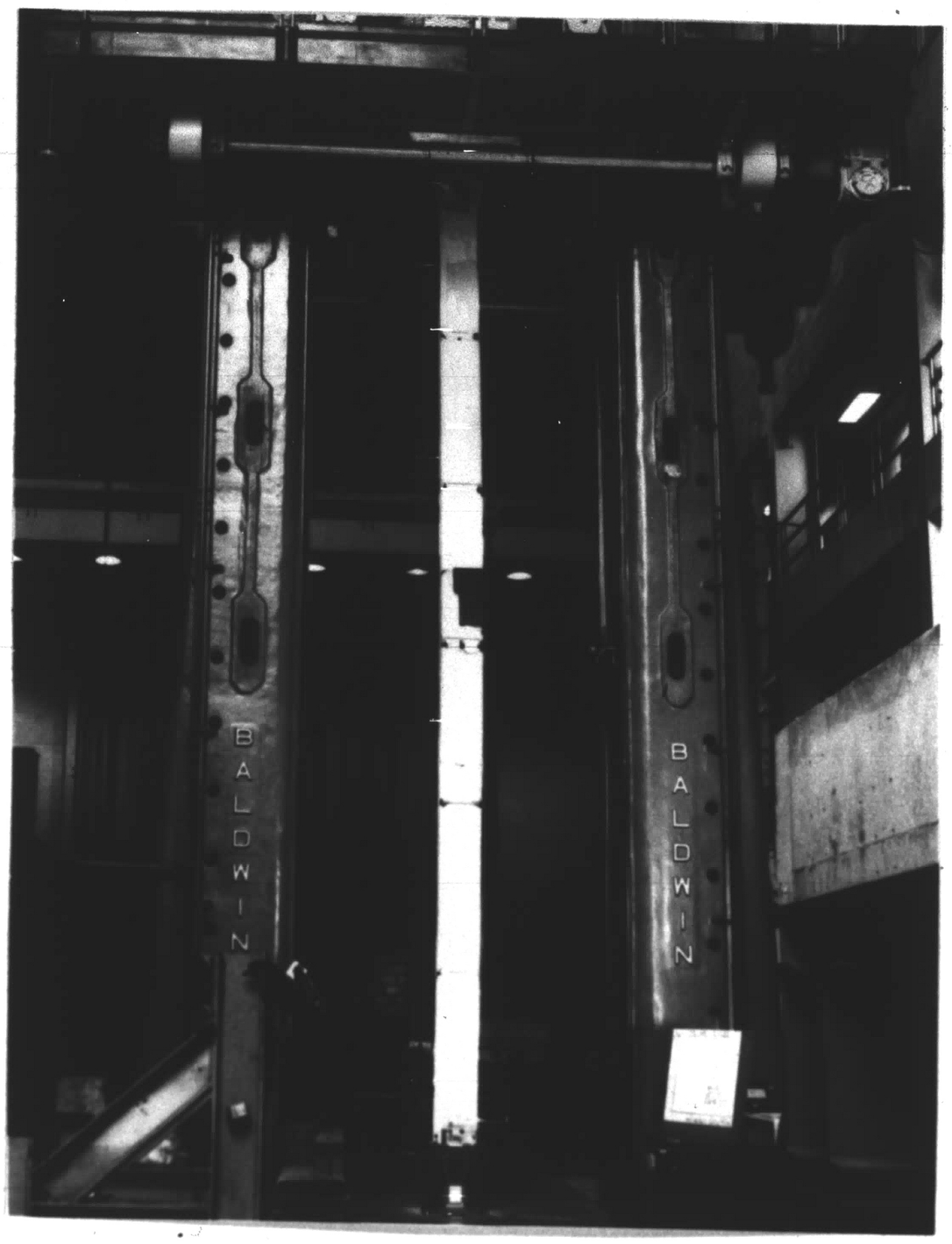

Fig. 32 Deflected Column: 4A, 14H202(FC), L/r = 90

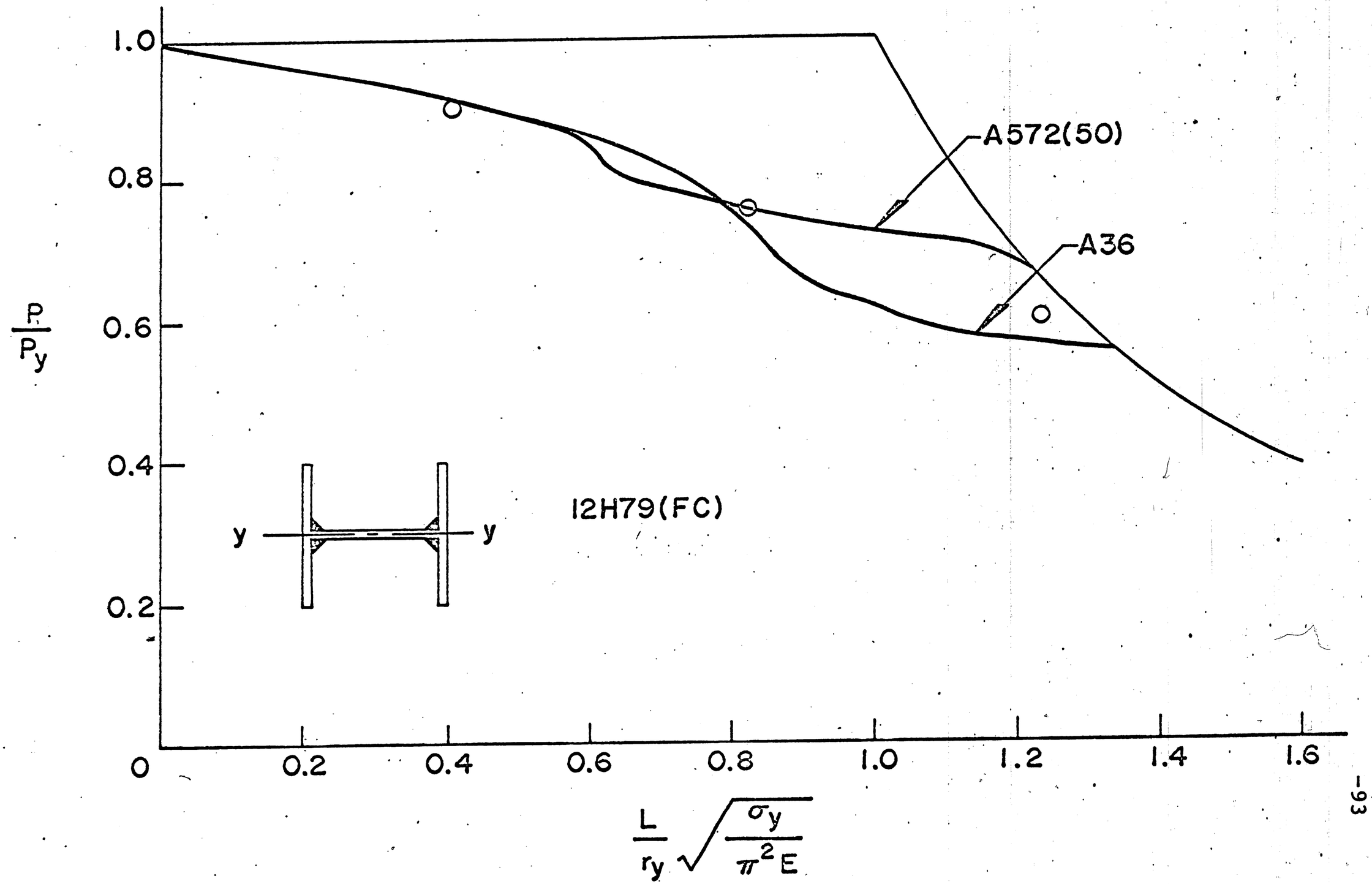

Fig. 33 Tangent Modulus Load Curve, 12H79(FC) -- Weak Axis

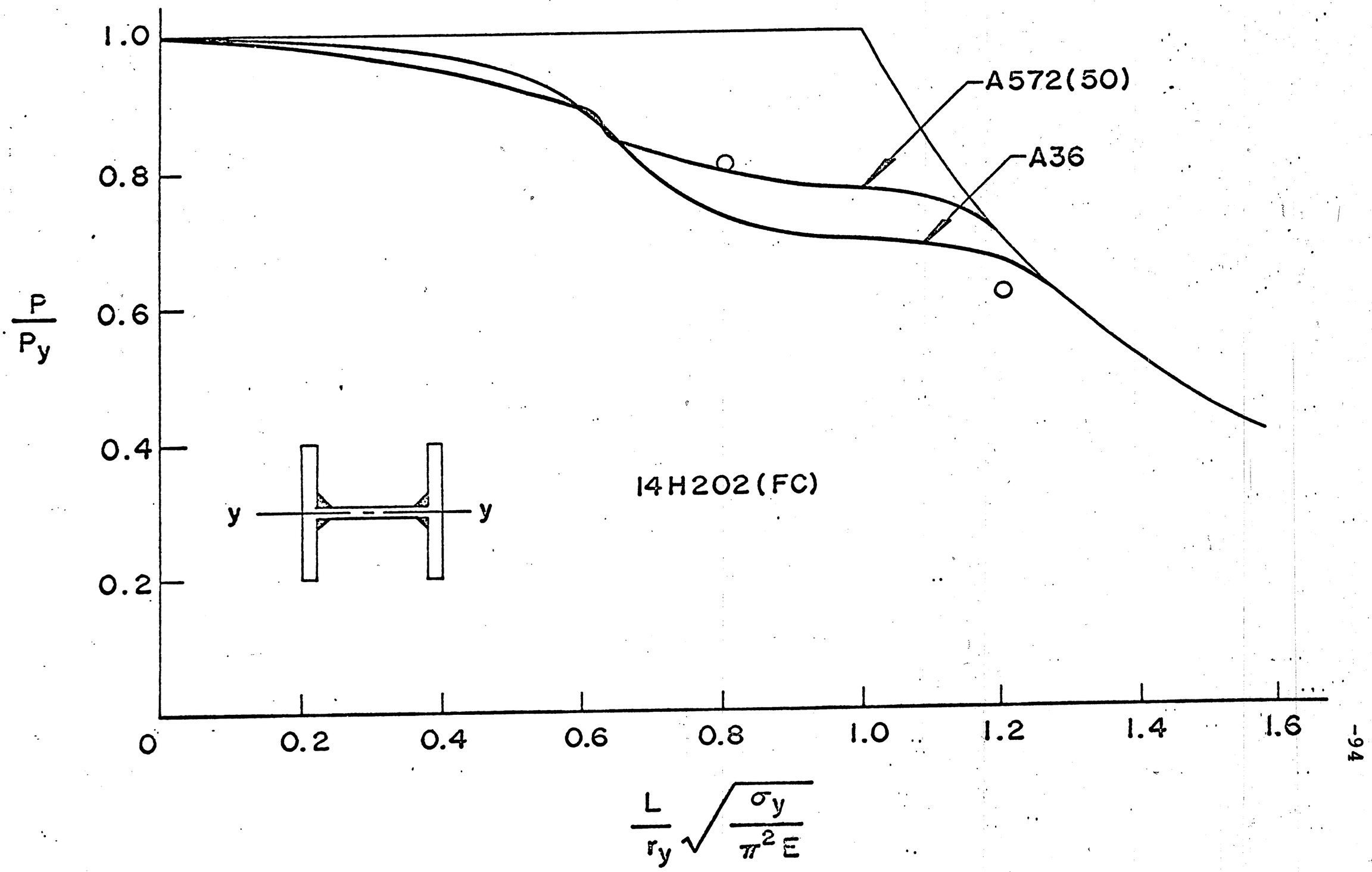

Fig. 34 Tangent Modulus Load Cirve, 14H202(FC) -- Weak Axis

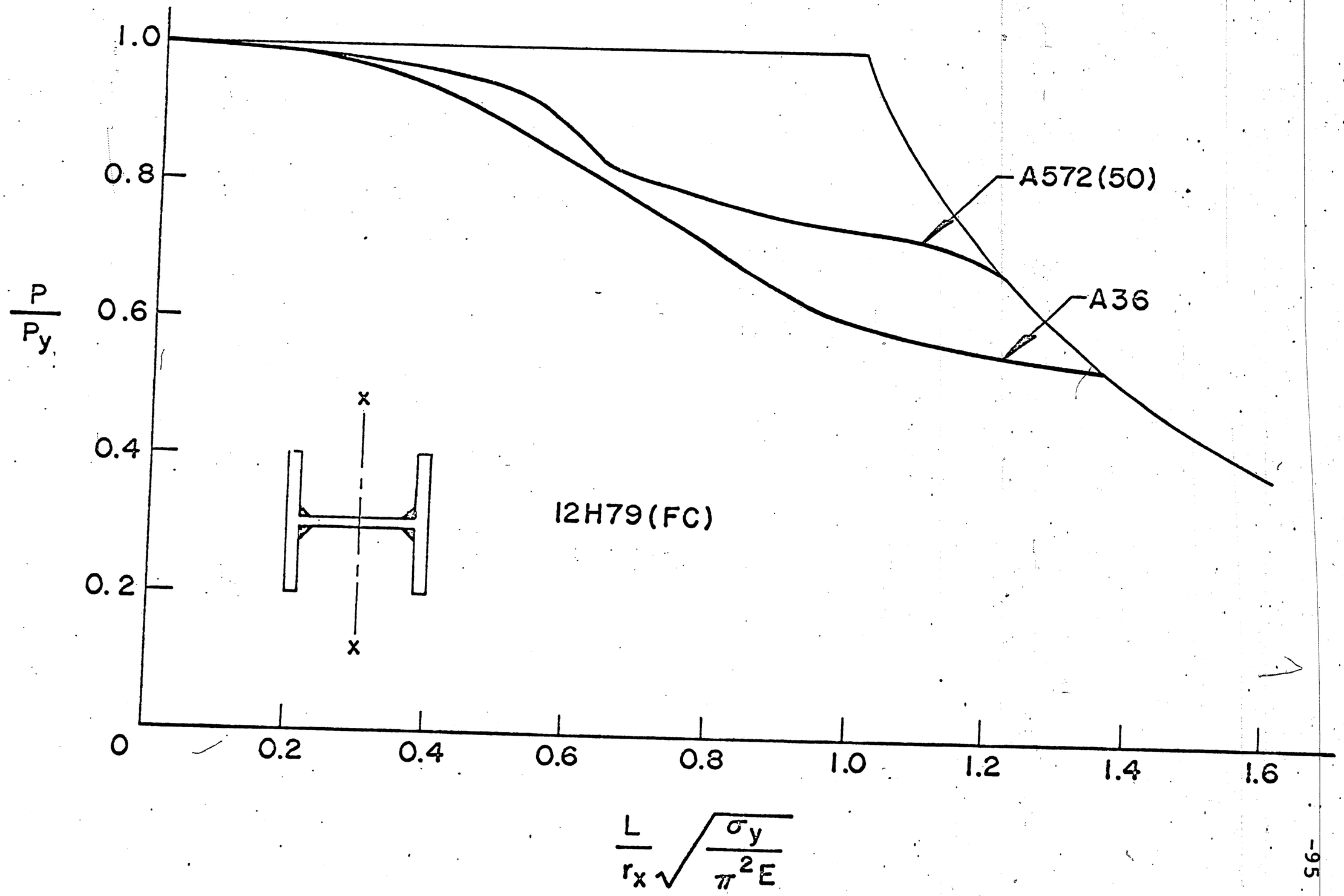

Fig. 35 Tangent Modulus Load Curve, 12H79(FC) -- Strong Axis

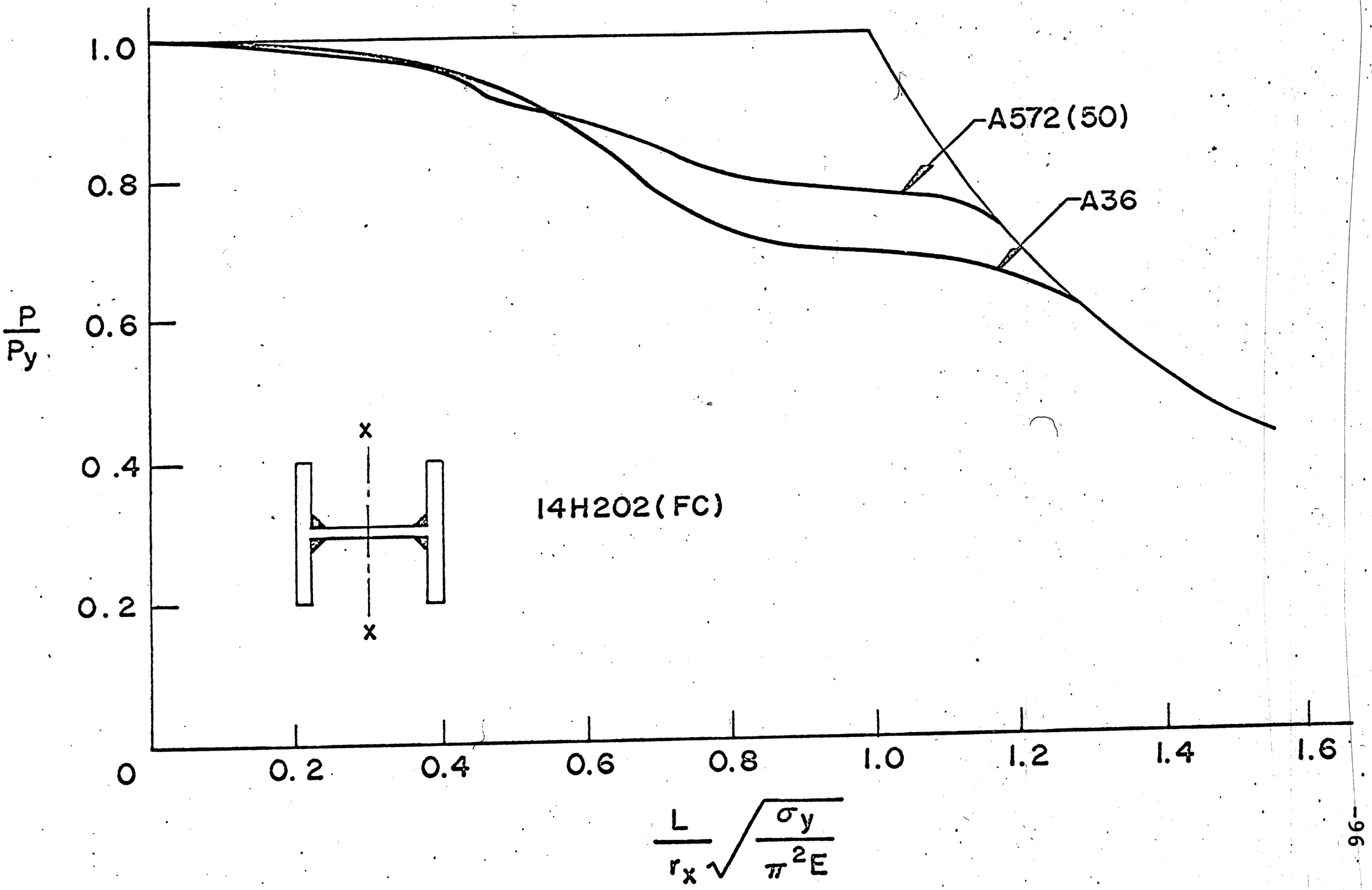

Fig. 36 Tangent Modulus Load Curve, 14H202(FC) -- Strong Axis

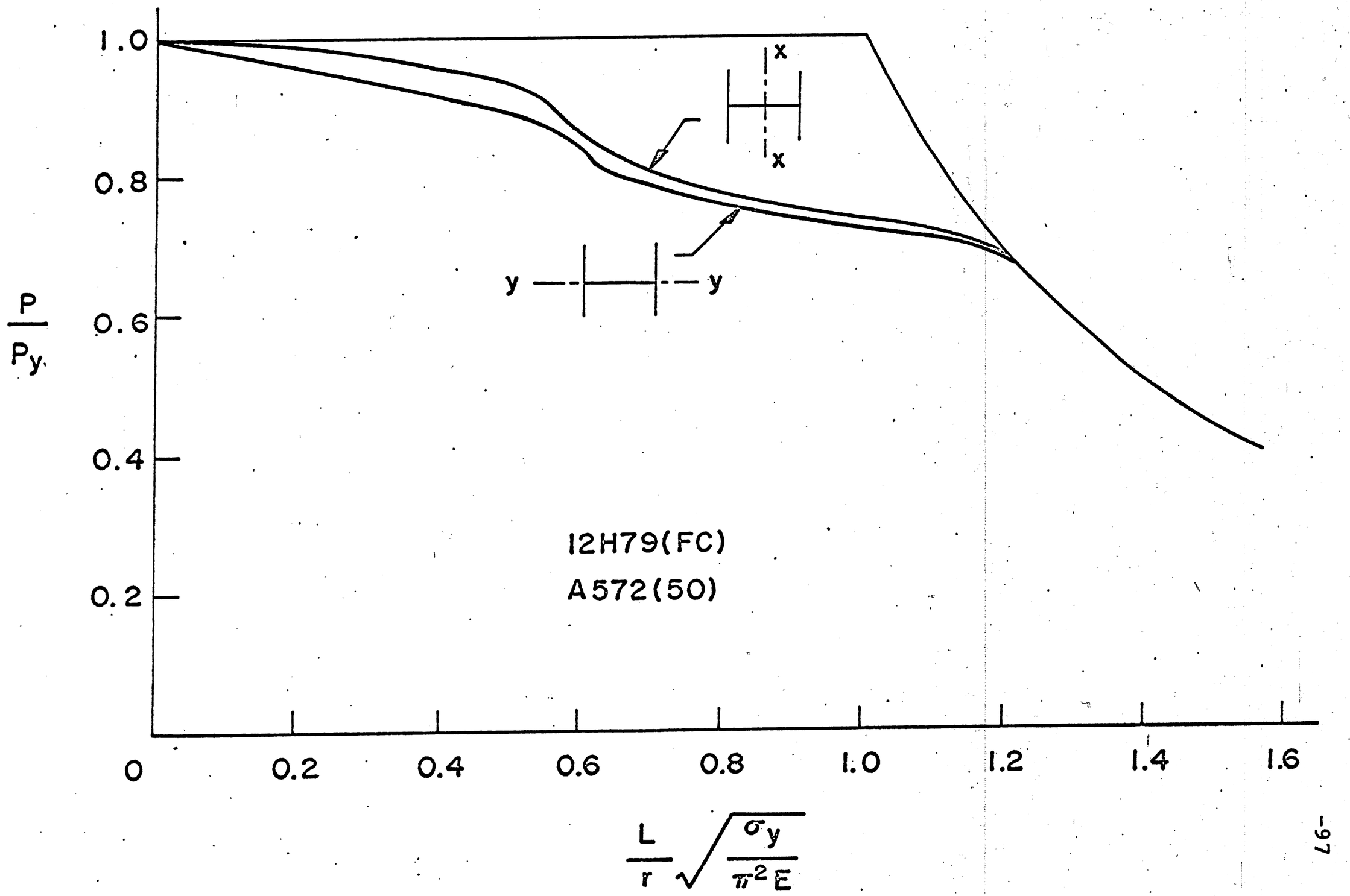

Fig. 37 Tangent Modulus Load Curves, 12H79(FC), A572(50) -- Strong and Weak Axes

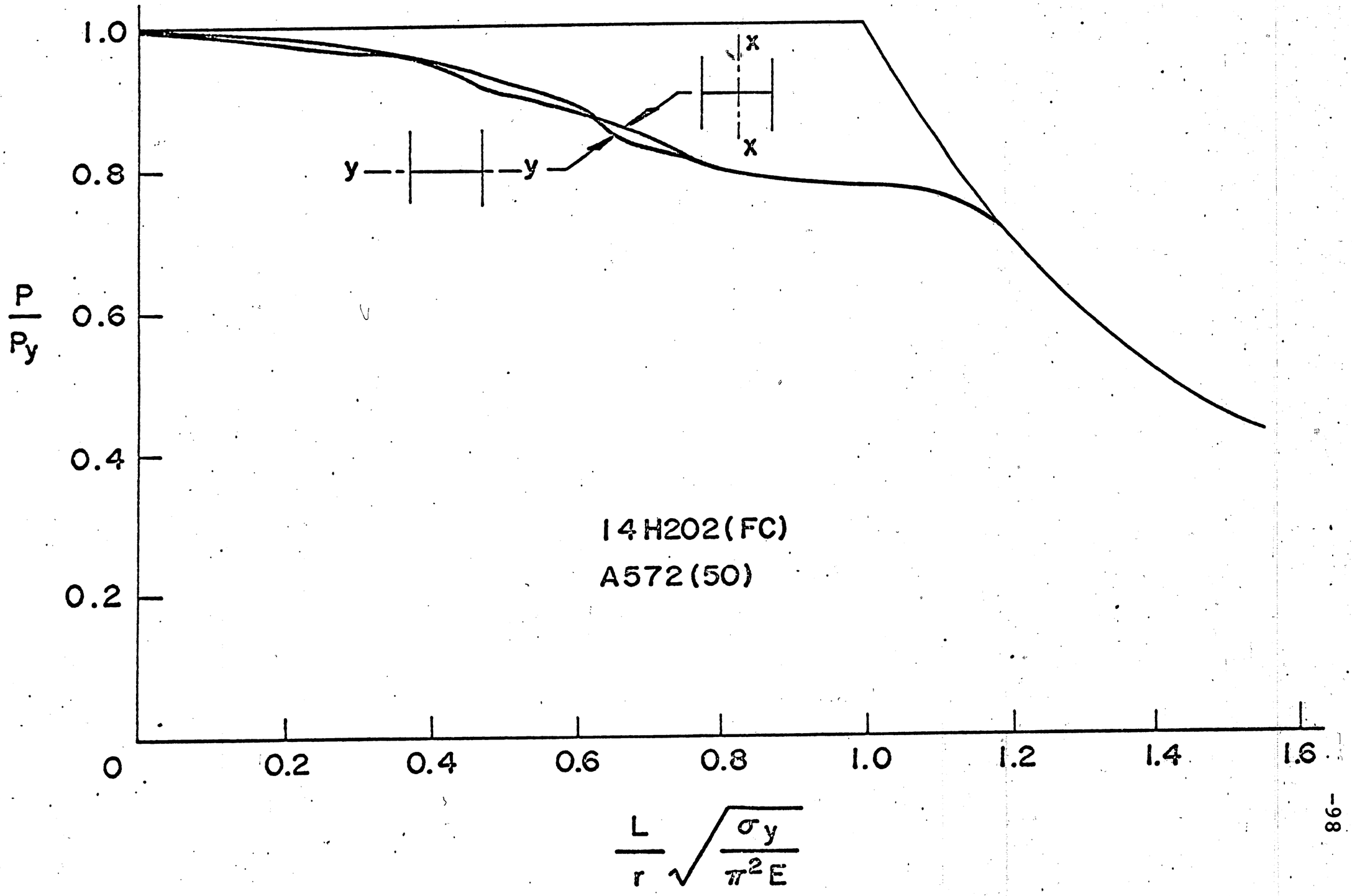

Fig. 38 Tangent Modulus Load Curves, 14H202(FC), A572(50) -- Strong and Weak Axes

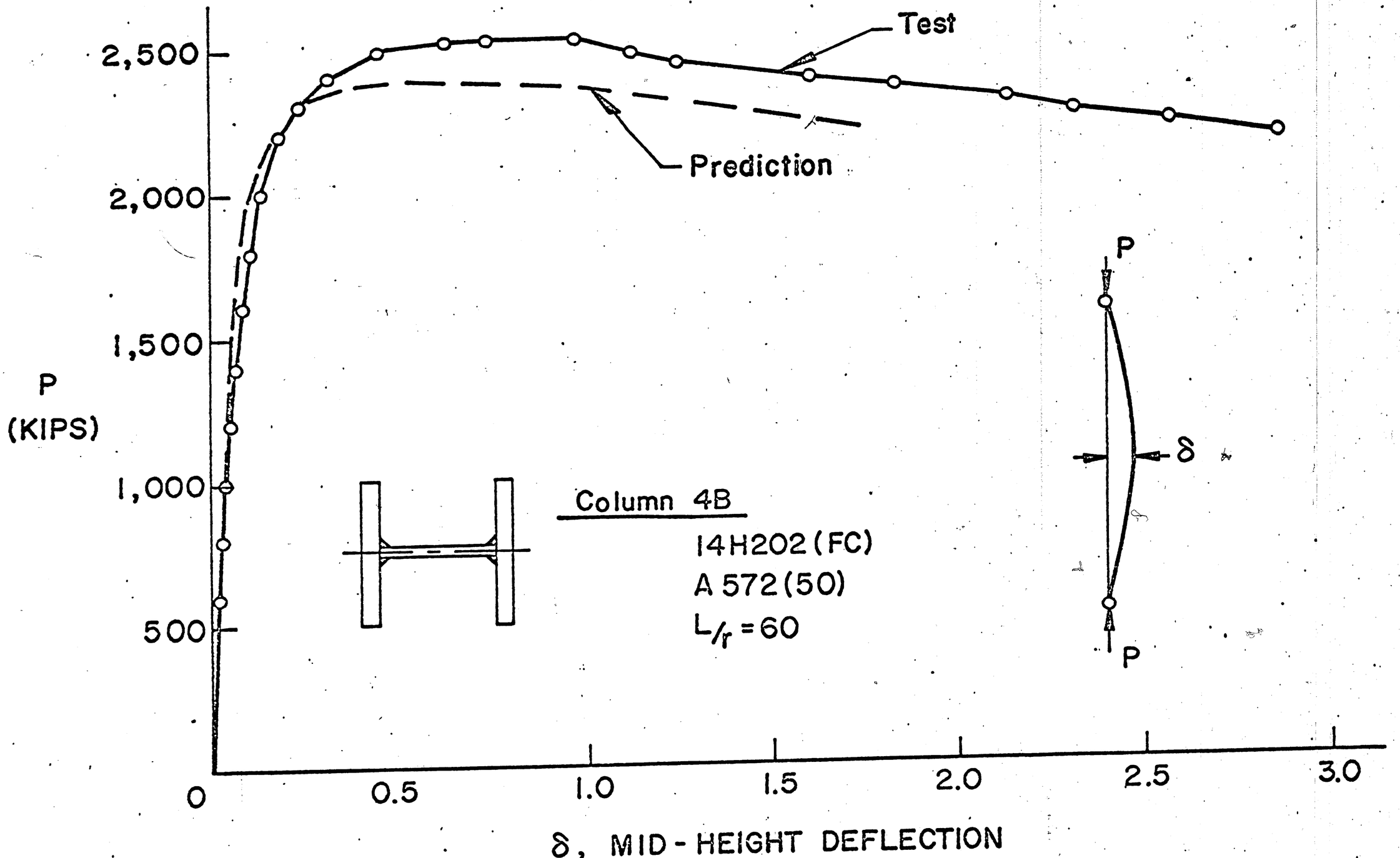

Fig. 39 Load-Deflection Curve for Ultimate Strength, Column 4B; 14H202 (FC), A572 (50), L/r = 60

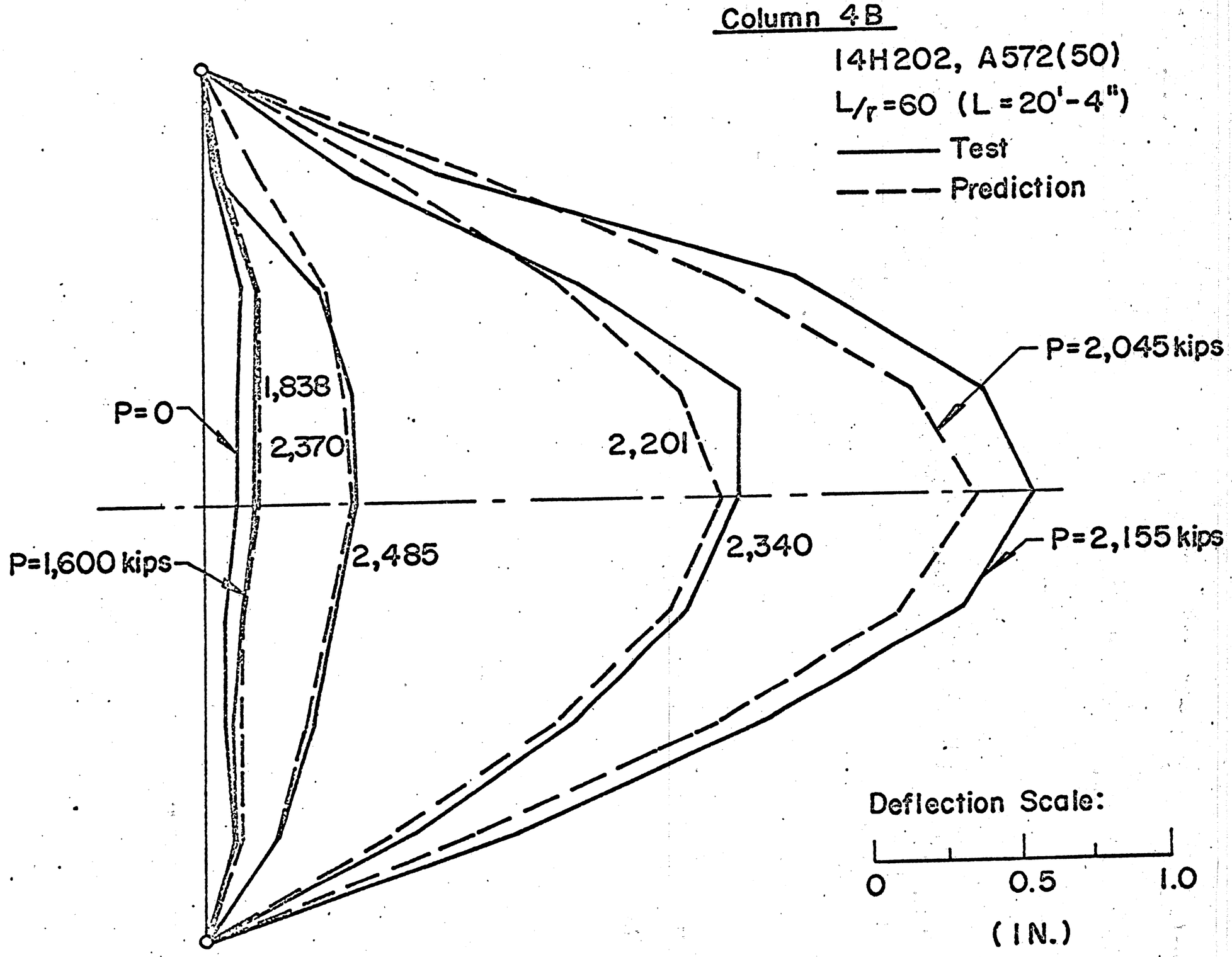

Fig. 40 Progress of Column Deflection, Column 4B; 14H202(FC), A572 (50), L/r = 60

10. REFERENCES

1. L.S. Beedle and L. Tall
BASIC COLUMN STRENGTH, ASCE, Proc., Paper 2555, Vol. 86, No. ST7, July 1960.

2. Y. Fujita
BUILT-UP COLUMN STRENGTH, Ph.D. Dissertation, Lehigh University, August 1956.

3. L. Tall
THE STRENGTH OF WELDED BUILT-UP COLUMNS, Ph.D. Dissertation, Lehigh University, May 1961.

4. F. R. Estuar and L. Tall
EXPERIMENTAL INVESTIGATION OF WELDED BUILT-UP COLUMNS, The Welding Journal, AWS, Vol. 42, April 1963.

5. F. R. Estuar
WELDING RESIDUAL STRESSES AND THE STRENGTH OF HEAVY COLUMN SHAPES, Ph.D. Dissertation, Lehigh University, August 1965.

6. F. Nishino
BUCKLING STRENGTH OF COLUMNS AND THEIR COMPONENT PLATES, Ph.D. Dissertation, Lehigh University, August 1964.

7. L. Tall
WELDED BUILT-UP COLUMNS, Fritz Engineering Laboratory Report No. 249.29, April 1966.

8. R. K. McFalls
A STUDY OF WELDED COLUMNS MANUFACTURED FROM FLAME-CUT PLATES, The Welding Journal, AWS, April 1969.

9. ASTM
STANDARD SPECIFICATION FOR HIGH-STRENGTH LOW-ALLOY COLUMBIUM-VANADIUM STEELS OF STRUCTURAL QUALITY, ASTM Designation A572-68, ASTM Standards, Part 4, January 1969.

10. N. R. Nagaraja Rao, M. Lohrmann and L. Tall
EFFECT OF STRAIN RATE ON THE YIELD STRESS OF STRUCTURAL STEEL, Journal of Materials, ASTM, Vol. 1, No.1, March 1966.

11. A. W. Huber and L. S. Beedle
RESIDUAL STRESS AND THE COMPRESSIVE STRENGTH OF STEEL, The Welding Journal, Vol. 33, No. 12, December 1954.

12. N. Tebedge
MEASUREMENT OF RESIDUAL STRESSES -- A STUDY OF METHODS, M.S. Thesis, Lehigh University, May 1969.

13. J. Brozzetti, G. A. Alpsten and L. Tall
ON THE ACCURACY OF THE SECTIONING METHOD FOR RESIDUAL STRESS MEASUREMENT, Fritz Engineering Laboratory Report No. 337.11 (In preparation).

14. CRC, Edited by B. G. Johnston
STUB COLUMN TEST PROCEDURE, Appendix, CRC, Guide to Design Criteria for Metal Compression Members, 2nd Edition, 1966.

15. A. W. Huber
FIXTURES FOR TESTING PIN-ENDED COLUMNS, ASTM Bulletin, No. 234, December 1958.

16. F. R. Estuar and L. Tall
TESTING OF PINNED-END STEEL COLUMNS, ASTM Special Technical Publication No. 419, p. 80, 1967.

17. N. Tebedge, P. Marek and L. Tall
COMPARISON OF COLUMN TESTING METHODS, Fritz Engineering Laboratory Report No. 351.2 (In preparation).

18. L. Tall
RECENT DEVELOPMENTS IN THE STUDY OF COLUMN BEHAVIOR, Journal of the Institution of Engineers, Vol. 36, No. 12, December 1964.

19. ASTM
STANDARD METHODS AND DEFINITIONS FOR MECHANICAL TESTING OF STEEL PRODUCTS, ASTM Designation A370-68, ASTM Standards, January 1969.

20. F. R. Shanley
INELASTIC COLUMN THEORY, Journal of Aeronautical Science, Vol. 14, pp. 261-267, May 1947.

21. CRC, Edited by B. G. Johnston
THE BASIC COLUMN FORMULA, Appendix, CRC, Guide to Design Criteria for Metal Compression Members, 2nd Edition, 1966.

22. C. H. Yang, L. S. Beedle and B. G. Johnston
RESIDUAL STRESS AND THE YIELD STRENGTH OF STEEL BEAMS, The Welding Journal, Research Supplement, Vol. 31, No. 4, p. 205, April 1952.

23. C. K. Yu and L. Tall
INELASTIC COLUMNS WITH RESIDUAL STRESSES, Fritz Engineering Laboratory Report No. 290.14, April 1968.

11. VITA

Yoshio Kishima was born in Peiping, China on August 21, 1941, the first son of Tsuneo Kishima and Iku Kishima.

He received his earlier education in Kyoto, Japan. He then attended Kyoto University, Kyoto, studying in the Department of Architecture, Faculty of Engineering, from 1961 to 1965. He received the degree of Bachelor of Science in Engineering in March 1965. He was a researcher in the Disaster Prevention Research Institute of the University from 1965 to 1966. Then he entered the Graduate School of Engineering of Kyoto University, majoring in Architectural Engineering. He completed the first year of the two-year program toward the degree of Master of Science in Engineering.

On May 10, 1967, he married Kazuko Katagishi in Kyoto.

In May, 1967, he joined the staff of Fritz Engineering Laboratory at Lehigh University as a

research assistant. Since then, he has been associated with the research project on "Welded Columns and Flame-Cut Plates" in the Structural Stability Division of the Fritz Engineering Laboratory.